Journal of Science and Technology
ISSN: 2456-5660 Volume 10, Issue 02 (Feb-2025)
www.jst.org.in *DOI:https://doi.org/10.46243/jst.2025.v10.i02.pp160-186*

Through an antioxidant mechanism, baicalein promotes remyelination and ameliorates motor dysfunction and cognitive impairment in an animal model of multiple sclerosis.

M. Kishore Babu[1], K. Balaram Kumar[2], L. Ramachandra Reddy[3], B. Sasidhar[4]

1.Professor, Department of pharmaceutics, QIS College of pharmacy, Ongole, A.P

2.Assosiate Professor, Department of pharmacogosy, QIS College of pharmacy, Ongole, A.P

3.Assistant Professor, Department of pharmacognosy, QIS College of pharmacy, Ongole, A.P

4 Assistant .Professor, Department of pharm.Biotech, QIS College of pharmacy, Ongole, A.P

To Cite this Article
M. Kishore Babu, K. Balaram Kumar, L. Ramachandra Reddy, B. Sasidhar, **"Through an antioxidant mechanism, baicalein promotes remyelination and ameliorates motor dysfunction and cognitive impairment in an animal model of multiple sclerosis.**" *Journal of Science and Technology, Vol. 10, Issue 02- Feb 2025, pp160-186*

Article Info
Received: 29-12-2024 Revised: 06-02-2025 Accepted: 17-02-2025 Published: 27-02-2025

ABSTRACT: The hallmark deficits of multiple sclerosis (MS), a chronic inflammatory and neurodegenerative disease, are caused by recurrent demyelination that destroys remyelination and disrupts axonal conduction. Traditional Chinese medicines are becoming more and more popular as researchers look for new medications to treat multiple sclerosis.

Techniques: In animal studies, C57BL/6J male mice were given cuprizone (CPZ), a copper chelator harmful to cell mitochondria, to create an animal model of multiple sclerosis. By looking at how baicalein (BA) affected the neuropathological alterations and behavioral abnormalities brought on by CPZ, the therapeutic benefits of BA were thoroughly examined. Additionally, the molecular and cellular processes that underlie BA's therapeutic actions were investigated. The OLN-93 cell line and cultivated oligodendrocyte (OL) lineage cells were used in the in vitro tests under different CPZ, H2O2, and BA conditions. Cell biology and biochemical techniques were used to assess the cultivated cells' survival, development, and mitochondrial activity as well as any oxidative stress indicators.

Findings: In the in vivo tests, BA promoted the remyelination process and reduced neuroinflammation in the brains of CPZ-exposed mice, aiding in the recovery of their motor and cognitive deficits. Underpinning these protective effects, BA's antioxidant activities kept the signal pathway at normal levels by preventing the over-activation of nuclear factor erythroid 2-related factor 2 (NRF2) and its downstream antioxidant enzymes (HO-1, NQO1, and SOD2). The in vitro tests demonstrated that CPZ and H2O2 both cause oxidative stress and damage to the cell's mitochondria, which delays the formation of oligodendrocyte (OL) lineage cells. By scavenging ROS produced by the cells' damaged mitochondria, BA successfully stopped the development delay of cultivated OLs.

Corresponding Author: M.Kishore Babu
Mail: kishorebabu.m@gmail.com

Conclusion: By promoting future therapeutic uses of BA in the treatment of MS patients, our studies show that BA's antioxidant properties promote remyelination and the growth of OL lineage cells in the MS model of CPZ-exposed mice.

KEYWORDS

baicalein, cuprizone, demyelination, mitochondria, oligodendrocytes, remyelination

1 Background

Demyelination, neuroinflammation, gliosis, and neurodegeneration are the main neuropathological alterations in the central nervous system (CNS) of multiple sclerosis (MS), a chronic inflammatory and neurodegenerative illness (Tobore, 2020). Motor dysfunction and cognitive impairment, such as slowed information processing speed, concentration problems, and long-term episodic memory are among the many clinical symptoms that MS patients may have (Woo et al., 2024). MS affects around 2.8 million individuals globally, with young adults between the ages of 20 and 30 being the most vulnerable group (Walton et al., 2020). T-lymphocyte-mediated inflammation is thought to be a key factor in the pathophysiology of multiple sclerosis (MS), which includes oxidative stress and mitochondrial dysfunction (Bargiela and Chinnery, 2019; Corthay, 2006; Gambini and Stromsnes, 2022; McGarry et al., 2018), as well as inflammation of the gray and white matter, myelin sheath destruction, and impaired remyelination (Tanaka et al., 2020; Zarghami et al., 2021). The most widely used experimental model for multiple sclerosis is experimental autoimmune encephalomyelitis (EAE), which is linked to the inflammation caused by T cells in MS. Cuprizone (CPZ), a copper chelator toxic to cell mitochondria, has been shown to cause demyelination and subsequent remyelination in the mouse brain, making it a useful animal model of multiple sclerosis (MS), in keeping with the mitochondrial dysfunction and oxidative stress (OS) associated with the disease (Abdel-Maged et al., 2020; Zirngibl et al., 2022).

According to Signorile et al. (2020), mitochondria are very sensitive to a variety of biological signals, including OS, and are essential for controlling apoptosis. In MS patients, mitochondrial dysfunction has been found in oligodendrocytes (OLs) and immune cells (López-Muguruza and Matute, 2023). While astrocytes and microglia were stimulated in mice exposed to CPZ, mitochondria in OLs were more vulnerable to the chemical's harmful effects (Luo et al., 2020; Yang et al., 2020b). These earlier findings suggest that OS and neuroinflammation are closely related in the pathophysiology of MS. under fact, under pathological circumstances of the central nervous system, glial and infiltrating immune cells are thought to be important generators of reactive oxygen species (ROS) and reactive nitrogen species (RNS) (D'Ambrosi et al., 2018).

Since 1993, when IFN-β1b was authorized by the FDA for use in

A rising variety of medicines have significantly transformed the management of relapsing forms of multiple sclerosis (MS) (Paty and Li, 1993). However, patients must deal with the increased and sometimes severe risks of side effects from active disease-modifying medications. For instance, patients with active radiographic illness throughout the two years on the medication had a dismal prognosis, according to long-term follow-up of patients in a pivotal study of intramuscular IFN-β1a (Bermel and Inglese, 2012). MS patients receiving treatment with

Journal of Science and Technology
ISSN: 2456-5660 Volume 10, Issue 02 (Feb-2025)
www.jst.org.in *DOI:https://doi.org/10.46243/jst.2025.v10.i02.pp160-186*

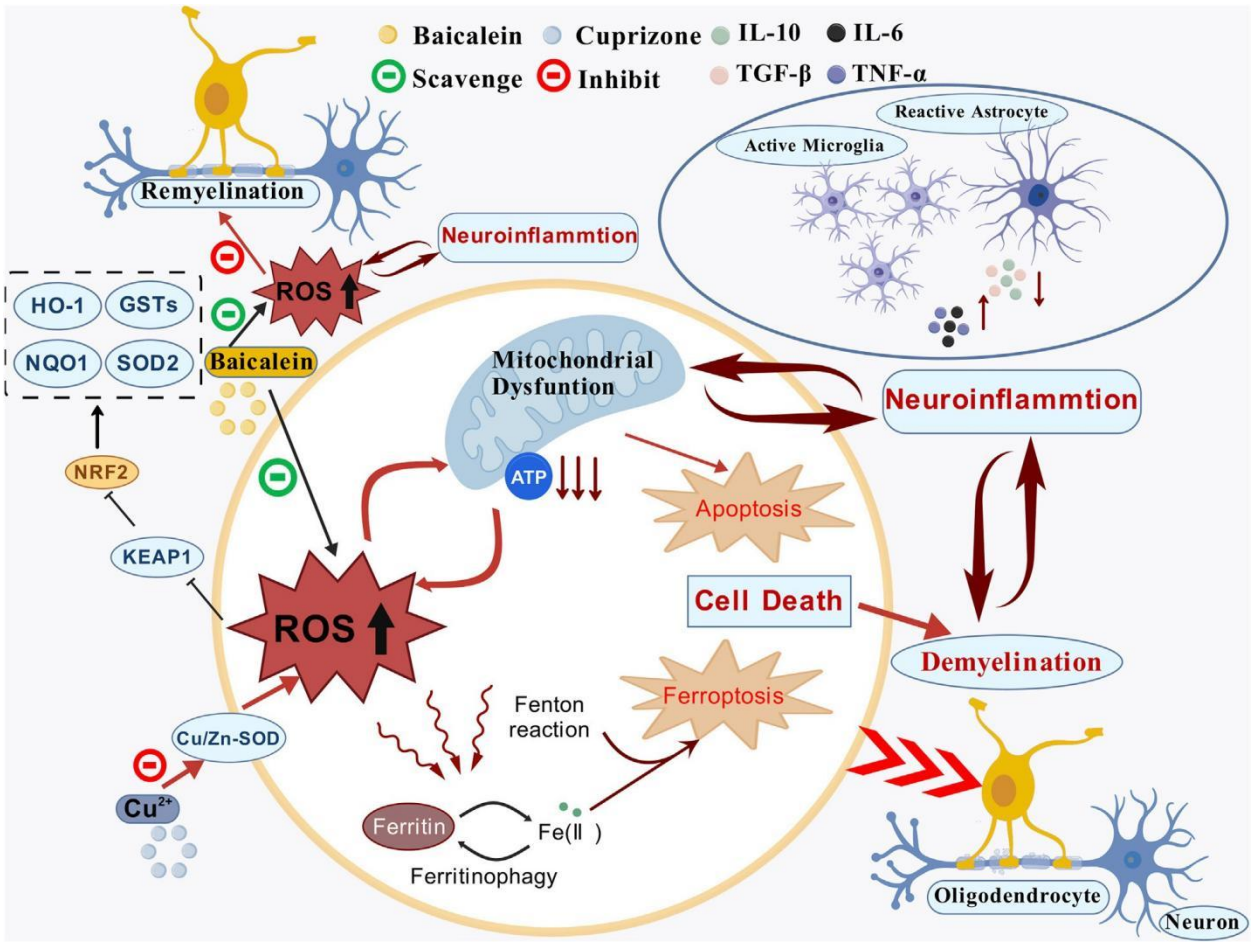

GRAPHICAL ABSTRACT

While natalizumab (Tysabri), a monoclonal antibody that targets the α4 integrin, inhibits the inflammatory elements of multiple sclerosis, its main adverse effect is progressive multifocal leukoencephalopathy (PML) (Langer-Gould et al., 2005; Morrow et al., 2022; Polman, 2006; Rudick et al., 2006). With 55%–60% lower relapse rates and a remarkable decrease in MRI-visible activity, the other second-era medication, fingolimod, has been shown to suppress MS disease activity (Cohen et al., 2010; He et al., 2015; Kappos et al., 2010; Pelletier and Hafler, 2012). However, it may cause lymphopenia as a side effect linked to varicella zoster virus (VCV) reactivation (Tanaka, 2016).
Antioxidant chemicals are becoming more and more popular in the hunt for novel medications to treat multiple sclerosis. The functions of naturally occurring or compounded derivatives of natural substances with well-known antioxidant potential in modulating the course of multiple sclerosis were compiled in a recent literature study (Theodosis-Nobelos and Rekka, 2022). Research indicates that these natural substances play a significant part in the pathophysiology of multiple sclerosis by either slowing down the disease's progression or improving some of its clinical symptoms, including fatigue, paralysis, and cognitive dysfunction, as well as by significantly lowering a number of oxidative and inflammatory markers. In order to build novel therapy or co-treatment options for multiple sclerosis, these earlier discoveries prompted more research on antioxidant chemicals or naturally derived compounds with multi-targeting and disease-modulating potential.

Scutellaria baicalensis Georgi (SBG) roots are the source of the flavonoid extract baicalein. Although it has no harmful effects over the wide range of studied levels, it shows considerable neuroprotective properties. SBG root is a traditional, suitable ingredient in herbal medicines used to treat central nervous system disorders. Consuming SBG has been linked in the past to a decreased risk of dementia and other age-related neurological conditions (Gasiorowski et al., 2011). Furthermore, by activating the transcription factor nuclear factor erythroid 2-related factor 2 (NRF2) and mediating the production of the antioxidant enzyme Mn-SOD, BA has been demonstrated in prior studies to scavenge superoxide and hydroxyl radicals and alleviate mitochondrial dysfunction (Licht-Mayer et al., 2015). BA prevented the migration of autoimmune T cells into the central nervous system and dramatically reduced the clinical severity of EAE in mice (Xu J. et al., 2013). BA reduced glial activation, pro-inflammatory cytokine production, demyelination, and motor impairment in mice exposed to CPZ, indicating that BA might be a helpful treatment for demyelinating illnesses like multiple sclerosis (MS) (Hashimoto et al., 2017).
Based on earlier research, we postulated that BA's antioxidant activity would shield OLs from CPZ's harmful effects on OL lineage cell development, hence accelerating the remyelination process in mice exposed to CPZ. Experiments using cultivated OLs and C57BL/6J mice were conducted to test this theory. In the animal studies, we investigated the neurobiological mechanisms behind BA's protective effects, assessed its potential to aid in the mice's recovery from behavioral abnormalities brought on by CPZ exposure, and looked at how BA affected remyelination and OL development in CPZ-exposed mice. By preserving the cells' mitochondrial activity, we showed that BA prevents CPZ and H2O2 from inhibiting the growth of OL lineage cells in cultivated OLs and OLN-93 cells.

2 Materials and methods

2.1 Reagents and chemicals

Cuprizone (purity >99%) and D-biotin were purchased from Sigma (St. Louis, Missouri, United States). B27 Plus was from Thermo Fisher (Waltham, Massachusetts, United States). ELISA kits for the assessment of IL-6, TNF-α, IL-10, TGF-β, NRF2, HO-1, NQO1, and SOD2 were from Keduo Di Biotechnology (Fujian, China). Fetal bovine serum (FBS), Dulbecco's Modified Eagle Medium (DMEM), DMEM/F-12, penicillin/streptomycin (P/S) solution and Accutase were purchased from Gibco (Carlsbad, California, United States). b-FGF and PDGF-AA were purchased from Peprotech (New Jersey, United States). Bovine serum albumin (BSA), Triton X-100, JC-1, CCK8, and ROS assay kits were from Beyotime Biotechnology (Shanghai, China). Sterile PBS buffer, sodium citrate repair solution, RIPA lysis buffer, corticosterone and triiodothyronine were purchased from Solarbio (Beijing, China). PVDF membrane was purchased from Millipore (Billerica, Massachusetts, United States). BCA protein assay kit and ECL exposure solution were purchased from NCM Biotech (Suzhou, China). The suppliers and catalog numbers

of all primary and second antibodies used in this study are presented in Table 1.

2.2 Experimental design and animal groups

This study consists of experiments with C57BL/6J male mice and cultured OL lineage cells. The C57BL/6J male mice in 7 weeks old were provided by Zhejiang Viton Lihua laboratory Animal Technology Co., Ltd. After an adaptation period of 7 days, all mice were randomly assigned into each of the following five groups: Control group (CNT), in which mice were fed standard mouse chow for 6 weeks without any additional intervention; CPZ+S group, in which mice were fed standard mouse chow containing 0.2% (w/w) cuprizone for 4 weeks, followed by administration of sterile saline (0.9%, gavage feeding at 1.0 mL/ 100 g body weight) for 2 weeks; and the other three groups in which mice were given BA at 10, 20, or 40 mg/kg in the same volume (1.0 mL/100 g body weight) of sterile saline as that in CPZ+S group. These three groups were referred to as CPZ+BA10, CPZ+BA20, or CPZ+BA40, respectively. By referring to a previous animal study (Li Y. et al., 2021), we chose the above doses of BA in this study. The CPZ+BA10 group consisted of 12 mice in two batches, each of the other four groups consisted of 17 mice in three batches.

After behavioral tests, mice of each group were euthanized and
their brains were subjected to the further analyses of immunofluorescence staining, Western blotting, and ELISA, in three subgroups, each of 5 or 6. In the data analyses, outliers that have a value exceeding 1.5 SD of the group average were prevented from further statistical analysis. This manipulation led to the uneven numbers in different analyses for the same animal groups.

The *in vitro* experiments were done with primary OL cultures or OLN-93 cell line, a rat OPC cell line obtained from BeNa Culture Collection (Hebei, China). For primary OL cultures, pregnant SD rats (Zhejiang Viton Lihua laboratory Animal Technology Co., Ltd.) were used.

TABLE 1 The suppliers and catalog numbers of antibodies used in the study.

Antibodies	Suppliers	Catalog number
Mouse anti-IBA1	Abcam	ab178846
Mouse anti-Olig2	Abcam	ab109186
Mouse anti-OXPHOS	Abcam	ab110413
Rabbit anti-APC	Abcam	ab40778
Rabbit anti-MBP	Abcam	ab40390
Rabbit anti-MOG	Abcam	ab32760
Goat anti-rabbit antibody Alexa Fluor 488	Abcam	ab150077
Mouse anti-GAPDH	Proteintech	60004-1
Rabbit anti-NAT8L-	Proteintech	23841-1-AP
Mouse anti-GFAP-	Proteintech	60190-1
HRP-conjugated goat anti-mouse	Proteintech	SA00001-1
HRP-conjugated goat anti-rabbit	Proteintech	SA00001-2
Mouse anti-Olig4	Sigma	O7139
Goat anti-mouse antibody Alexa Fluor 488	Thermo Fisher	A-11001
Goat anti-rabbit antibody Alexa Fluor 594	Thermo Fisher	A-11012

The mice and pregnant SD rats were maintained in the SPF- grade animal facility of the School of Mental Health, Wenzhou Medical University. They were group-housed (six mice per cage) with free accesses to water and food. The animal facility was well- ventilated, with a constant temperature (22 ˚C ± 1 ˚C), in a humidity range of 50%–60%, and a 12 h/12 h light-dark cycle. All animal experimental procedures described in this study were following the guidelines on animal care and use of Wenzhou Medical University and approved by the Ethics Committee of Wenzhou Medical University (2023Y07M07D). All animal experiments followed the 3Rs principle, and animals suffering was minimized as much as possible throughout the experimental procedures.

2.3 Behavioral tests

2.3.1 Rotarod test

This is a classic test for evaluating motor coordination in rodents. Before the test, the starting speed of the rotarod device (YLS-4D, Nuolei Xinda Technology Co., Ltd., Tianjin, China) was set to 5 r/min, with a uniform accelerating speed from 5 r/ min to 50 r/min within 6 min. When tested, a mouse was placed on the rotarod with his forepaws attached to the horizontal bar. The time from the start of the test until the first time the mouse fell off the rod or turned around on the rod was recorded. If a mouse did not slip or flip over for more than 5 min, the first flip latency was recorded as 5 min. The experiment was repeated two times for each mouse at an interval of 15 min, and the average value of the two latencies was finally used to evaluate the motor coordination ability of the mouse. After each experiment, the rotarod was wiped clean with 75% alcohol to eliminate the odor from a previous mouse.

2.3.2 Y-maze test

The Y-maze consisted of three identical arms radiating outward from the joint area at an identical angle of 120 ° between two arms. All arms had the same dimensions of 30 cm (length), 8 cm (width), and 15 cm (height). Mice were acclimated to the behavioral laboratory environment for 1 day before the test. During the test, a mouse was placed at the end of an arm and allowed to freely explore the Y-maze for 8 min, during which period the mouse's movement trajectory on the maze was recorded by a camera above the maze. After a test, the interior walls of the maze were cleaned with 75% alcohol to eliminate the odor from the tested mouse. Mice with normal spatial memory are expected to visit the three arms in a non-repetitive order, such as ABC, BCA, CAB, and so on. The total number of arm entries was recorded, and the percentage of the actual number of correct arm entries to the theoretical number of correct arm entries (total number of arm entries minus 2) is referred to as the spontaneous alternation rate (expressed as percentage).

2.3.3 Novel object recognition (NOR) test

The protocol described here was modified from that by Ennaceur and Delacour (Ennaceur and Delacour, 1988). The test was performed in a gray open-top cube empty box (with dimensions of 45 cm in length, width, and height) in 3 days. The apparatus was placed in a sound-isolated room.

The NOR procedure consisted of the habituation, training, and retention trials in 3 days. On the first day, mouse was habituated to the apparatus by exploring the test area in the absence of objects for 5 min. To avoid the presence of olfactory trails, the apparatus after each trial was thoroughly cleaned. On the second day, mouse was individually put back into the box and allowed to explore the same test area in the presence of two identical objects for 10 min (training trial). Exploration of an object was defined as directing the nose to the object at a distance of maximum 1 cm and/or touching it with the nose. The objects could not be displaced by a mouse as they were stuck to the wall of the open field. After a 2 h rest period, the same mouse was subjected to another test (first retention trial) in which he explored two objects, a familiar one used in the training trial and a novel one on the same area for 5 min. On the third day, each mouse was subjected to the second retention trial as the first retention trial (exploring a familiar object and a novel one for 5 min). The order of objects used per subject per trial was determined randomly. All combinations and locations of objects were used in a balanced manner to reduce potential biases because of preferences for particular locations or objects.

The exploration time for the novel and familiar objects in the retention trials was recorded, and the recognition index (RI) was quantified as the preference for the novel object, with the formula: RI = (time exploring the novel object)/(time exploring the novel object + time exploring the familiar object).

2.4 Immunofluorescence staining

For brain tissue immunofluorescence staining (IFS), the mouse was anesthetized with 1.25% tribromoethanol at a dose of 2.0 mL/100 g body weight. Under the deep anesthesia, the mouse was transcardially perfused with the phosphate buffered saline (PBS, pH = 7.4) until the liquid flowing out of the right atrial appendage was clear and the liver turned white. Then the whole brain of mouse was removed out of the skull and post-fixed in 4% paraformaldehyde (PFA) at 4 ℃ for 3 days and subsequently transferred into 30% sucrose solution at 4 ℃ for 48–72 h. The brain samples were then cut into 30-μm-thickness cross- sections using a Leica cryostat (CM30505, Leica Microsystems, Wetzlar, Germany) for IFS. The procedures for IFS of the brain sections include:

1) brain sections were fixed in 4% PFA for 30 min, then placed in a1× sodium citrate solution at 95 ℃ for 30 min; 2) after cooling to room temperature, the sections were incubated with a mixture of 5% BSA and 0.3% Triton X-100 for 60 min at room temperature; 3) one of primary antibodies (Rabbit anti-MBP, 1:1,000; Mouse anti-Olig2, 1:500; Mouse anti-GFAP, 1:500; Rabbit anti-IBA-1, 1:1,000) was applied and incubated overnight at 4 ℃ in a humidified chamber; 4) After rinsing with PBS 3 × 5 min, a second antibody (Goat anti-mouse secondary antibody Alexa Fluor 488, 1:1,000; Goat anti-rabbit secondary antibody Alexa Fluor 488, 1:1,000; or Goat anti-rabbit secondary antibody Alexa Fluor 594, 1:1,000) was applied and incubated for 60 min at room temperature; 5) the sections were mounted with a DAPI-containing mounting medium, dried, and observed under an inverted fluorescence microscope for imaging (LEICA DMI8, Wetzlar, Germany). The IFS images were analyzed using the ImageJ software (NIH, Bethesda, MD, United States).

The procedures of IFS for cultured oligodendrocyte linage cells include: 1) the slides with cultured cells (OLs) were rinsed with PBS 3× 5 min; 2) 4% PFA was added onto the slides to fix the cells for 15 min, followed by PBS rinsing three times; 3) the slides with OLs were immersed in 0.3% Triton X-100 for 10 min × 3; 4) the slides were immersed in 5% BSA for 60 min; 5) the slides were incubated with a primary antibody (Mouse anti-Olig2, 1:200; Mouse anti-Olig4, 1:200; Rabbit anti-

APC, 1:500) at 4 ℃ overnight; 6) after rinsing with PBS 3 times, the slides were incubated with a secondary antibody specific to a primary antibody for 60 min at room temperature; 7) after rinsing with PBS 3 times, the slides were sealed with a sealing agent containing DAPI; 8) observed under an inverted fluorescence microscope for imaging (LEICA DMI8, Wetzlar, Germany). The IFS images were analyzed using the ImageJ software.

2.5 Western blotting analysis

Tissue samples from the prefrontal cortex (PFC) and hippocampus (HIP) of mice were weighed and lysed with RIPA lysis buffer (1.0 mg in 1.0 mL), homogenized at 4 ℃, and centrifuged at 12,000 rpm for 15 min. The supernatant was collected, and protein concentration was measured. Equal amounts of protein (20 μg) were loaded onto each well of the 4% stacking gel and run onto the 10% SDS-polyacrylamide gel. Then the proteins were transferred from the separating gel to a PVDF membrane. The membrane was blocked with 5% skim milk for 1.5 h and incubated with a primary antibody overnight at 4 ℃. The primary antibodies used for the Western blotting experiments include rabbit anti-MBP (1:1,000), rabbit anti-MOG (1:1,000), mouse anti-total OXPHOS cocktail (1:250), mouse anti-GFAP (1:500), and rabbit anti-NAT8L (1:2,000), with the mouse anti- GAPDH (1:10,000) as the internal control. After rinsing the PVDF membrane with 1 × TBST (3 × 10 min), the membrane was incubated with a secondary antibody of horseradish peroxidase- conjugated goat anti-rabbit (1:10,000) or horseradish peroxidase- conjugated goat anti-mouse (1:10,000) for 1 h at room temperature. Finally, the membrane was developed using ECL exposure solution in a gel imaging system (VILBER, Paris, France), and the bands were quantified using ImageJ software.

2.6 Enzyme-linked immunosorbent assay (ELISA) of cytokines

Tissue samples from the PFC and HIP of mice were weighed and homogenized in PBS (100 mg tissue added into 900 μL PBS). The homogenate was centrifuged at 3,000 rpm, 4 ℃, for 20 min and the supernatant was collected. 50 μL of the prepared samples and standards were added to each well of an ELISA plate, followed by the addition of 50 μL biotinylated antigen working solution and incubated at 37 ℃ for 30 min. After spilling out the solutions, all wells were rinsed 5 times with PBS, then 50 μL of streptavidin-HRP working solution was added into each well and incubated at 37 ℃ for 30 min. After rinsing wells with PBS again, color development solutions A and B (50 μL each) were added into each well and incubated at 37 ℃ for 10 min. The reaction was stopped by adding 50 μL of stop solution, and the OD value was read out within 10 min at 450 nm using an ELISA microplate reader (TECAN Infinite M200 Pro, Switzerland). Protein levels of the inflammatory cytokines including IL-6, TNF-α, IL-10, and TGF-β were calculated using ELISA calc with a logistic curve (four-parameter) model.

2.7 Cell culture of primary oligodendrocytes and drug treatments

The cerebral cortex of newborn SD rats (0–2 days old) was used to harvest brain cells, which were then seeded onto poly-D-lysine-coated T75 culture flasks at a density of 1 × 106/cm2 and cultured at 37 °C in a CO2 incubator, according to a prior work (Xu H. et al., 2013). Up to day nine in vitro (DIV9), the media was switched every three days. To separate the microglial cells, the T75 flasks were shaken at 150 rpm for 60 minutes. The flasks were then shaken constantly for 15–20 hours at 250 rpm in order to separate astrocytes from oligodendrocyte precursor cells (OPCs). After that, adhering astrocytes and microglia were eliminated by transferring the media to culture plates and letting it settle for 60 minutes. The pellets were then resuspended and planted onto cell culture inserts or slides at the proper density after the media had been centrifuged for six minutes at 1,800 rpm. Following two days of culture in proliferation medium (DMEM supplemented with 2% B27 Plus, 0.5% FBS, 1% P/S, 0.1% PDGF-AA, and 0.1% b-FGF), the cells were moved to differentiation medium (DMEM/F12 supplemented with 0.5% FBS, 1% P/S, 1% nitrogen, 10 nM Corticosterone, 10 nM D-biotin, and 30 nM triiodothyronine) for additional culture.
OPCs were treated to 0.5 mM CPZ for 24 hours beginning on DIV11 in this experiment. Beginning with DIV13, differentiated OLs were exposed to CPZ for 24 hours. Beginning on DIV15, immature OLs were exposed to CPZ for 24 hours.

2.8 Cell culture of OLN-93 cell line

OLN-93, a rat OPC cell line, was obtained from BeNa Culture Collection (Hebei, China). The cells were cultured in DMEM

(supplemented with 10% FBS, 1% P/S) at 37 ˚C in a humidified atmosphere containing 95% air and 5% CO_2. Cells at 80%–90% confluence were selected for subculture and subsequent experimentation.

2.9 CCK-8 assay

WST-8 (Cell Counting Kit 8; CCK-8) has been accepted as a validated method for measuring the viability of cultured cells. It can be reduced by dehydrogenases in the mitochondria to produce an orange-yellow formazan in the presence of an electron coupling reagent. The color intensity is proportional to cell viability. In our experiment, extracted OL linage cells were cultured in 96-well plates until approximately 80% of the well area is covered by the cells. Then various concentrations of CPZ (0, 0.025, 0.05, 0.1, 0.5, 1.0, 2.0 mM) were added into the culture medium of primary OLs on DIV11-12, or various concentrations of H_2O_2 (0.2, 0.4, 0.8, or 1.6 mM) were added into the culture medium of OLN-93 cells when the cell density reaches 80%–90%. Both the culture conditions maintained for 24 h. Then the culture medium was removed, and the cells were washed once with PBS, followed by the addition of 100 µL fresh medium and 10 µL CCK-8 solution into each well. Furthermore, the plate was incubated in a CO_2 incubator for additional 2 h before absorbance measurement at 450 nm on the same microplate reader as mentioned above. Each group was prepared in 6 wells at least 3 independent experiments. The relative cell viability was expressed as a percentage of the control cells that were treated neither with CPZ nor with H_2O_2.

2.10 Assessment of mitochondrial membrane potential

During the early stage of differentiation (DIV13-DIV14), primary OPCs were treated with CPZ (0, 0.5 mM) and BA (0, 20 μM (Kim et al., 2023)) for 24 h, then the culture medium was removed from the confocal culture dishes, and the cells were washed once with PBS and then stained by a mixture solution consisting of equal volume (each of 1.0 mL) of culture medium and JC-1 staining working solution at 37 ˚C for 20 min. After incubation, the supernatant was removed, and the cells were washed twice with JC-1 staining buffer. Then 2.0 mL of culture medium was added, and the cells were observed under a laser confocal microscope (LEICA DMI8, Wetzlar, Germany). The relative degrees of mitochondrial polarization were quantified by measuring the red-shifted JC-1 at 535 nm (Ex) and 590 (Em) and green shifted JC-1 at 515 nm (Ex) and 529 nm (Em).

2.11 Detection of ROS

Intracellular ROS can oxidize non-fluorescent DCFH to fluorescent DCF, allowing the detection of ROS levels based on fluorescence intensity. In brief, when the cell density reaches 80%– 90%, the OLN-93 cells were treated with H_2O_2 (0, 400 μM) and BA (0, 40 μM (Kim et al., 2023)) for 24 h. Then the original culture medium was removed, followed by the addition of diluted DCFH- DA (10 μM/L) into the cell-containing wells. After incubation at 37 ˚C for 20 min, the cultures were rinsed three times with serum- free culture medium. Finally, the ROS levels were detected using a fluorescence microplate reader (LEICA DMI8, Wetzlar, Germany).

2.12 Statistical analysis

SPSS 25 was used to analyze the data. Data conforming to a normal distribution were expressed as mean ± standard error of the mean (Mean ± SEM). Levene's test was used to assess homogeneity of variance. For data in multiple groups, one-way ANOVA or repeated-measures ANOVA was used to evaluate the effects of experimental treatments, followed by LSD multiple comparisons for group-wise comparisons. For comparisons between two groups, t-tests were used, with $p < 0.05$ indicating statistical significance. GraphPad Prism 9 was used for graphing. Each experiment was repeated at least three times.

3 Results

3.1 Baicalein improved motor dysfunction and cognitive impairment in cuprizone- exposed mice

In the rotarod test, the mice in the five groups performed differently in terms of the first flip latency (Figure 1A). One-way ANOVA of the results indicated a significant main effect of grouping ($F = 12.27$, $p < 0.0001$). Post-hoc tests reported a significant difference between CNT and CPZ+S groups in the first flip

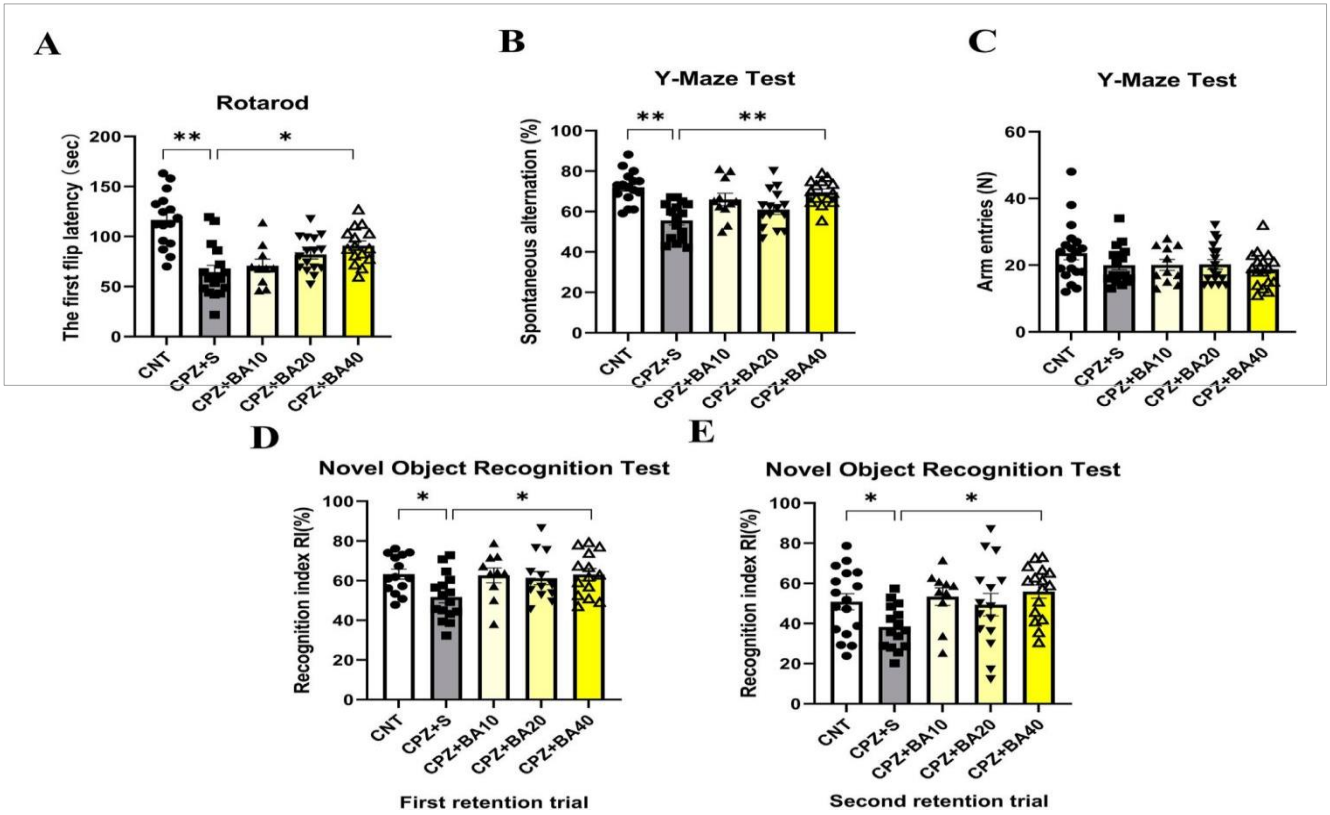

latency ($p < 0.0001$). The differences also existed between CNT and CPZ+BA10 ($p < 0.0001$)/BA20 ($p = 0.0005$)/BA40 ($p = 0.0191$) groups. Moreover, the CPZ+BA40 group showed a significantly longer first flip latency relative to the CPZ+S group ($p = 0.0159$). In the Y-maze test, the mice in the five groups also performed differently (Figures 1B,C). One-way ANOVA of the spontaneous alternation revealed a significant main effect of grouping ($F = 9.295$, $p < 0.0001$). Post-hoc tests reported that the spontaneous alternation in the CPZ + S group was significantly lower than that in the CNT group ($p < 0.0001$), but no significant difference existed between CNT and CPZ+BA40 groups. Moreover, CPZ+BA40 group exhibited a significant higher spontaneous alternation compared to the CPZ+S group ($p = 0.0003$). Interestingly, one-way ANOVA of
the arm entries data showed no significant effect of grouping.

In the novel object recognition test, mice in all five groups performed differently in terms of RI in the two retention trials. For the first retention trial (done 2 h after the training trial), one-way ANOVA revealed a significant effect of grouping on RI ($F = 3.244$, $p = 0.0298$). Post-hoc tests reported a significant lower RI in the CPZ+S group compared to the CNT group ($p = 0.0464$). It was also significantly lower than that in the CPZ+BA40 group ($p = 0.0442$). But there was no difference between any other two groups (Figure 1D). Same results were also found in the second retention trial, i.e., the main effect of grouping is significant on RI ($F = 3.754$, $p = 0.0162$), significant differences existed between CNT and CPZ+S groups ($p = 0.0177$), between CPZ+S and CPZ+BA40 groups ($p = 0.0129$) (Figure 1E).

3.2 Baicalein promoted remyelination following CPZ-induced demyelination in mice

Figure 2A shows representative MBP IFS images taken at cerebral cortex of the mice from the three groups of CNT, CPZ+S, and CPZ+BA40. Close observation of these images at a higher magnification tells obvious differences in terms of MBP immunostaining in the mice. Consistent with this visual observation, grouping showed a significant effect on the MFI of MBP ($F = 5.440$, $p = 0.0192$). Post-hoc comparisons reported that

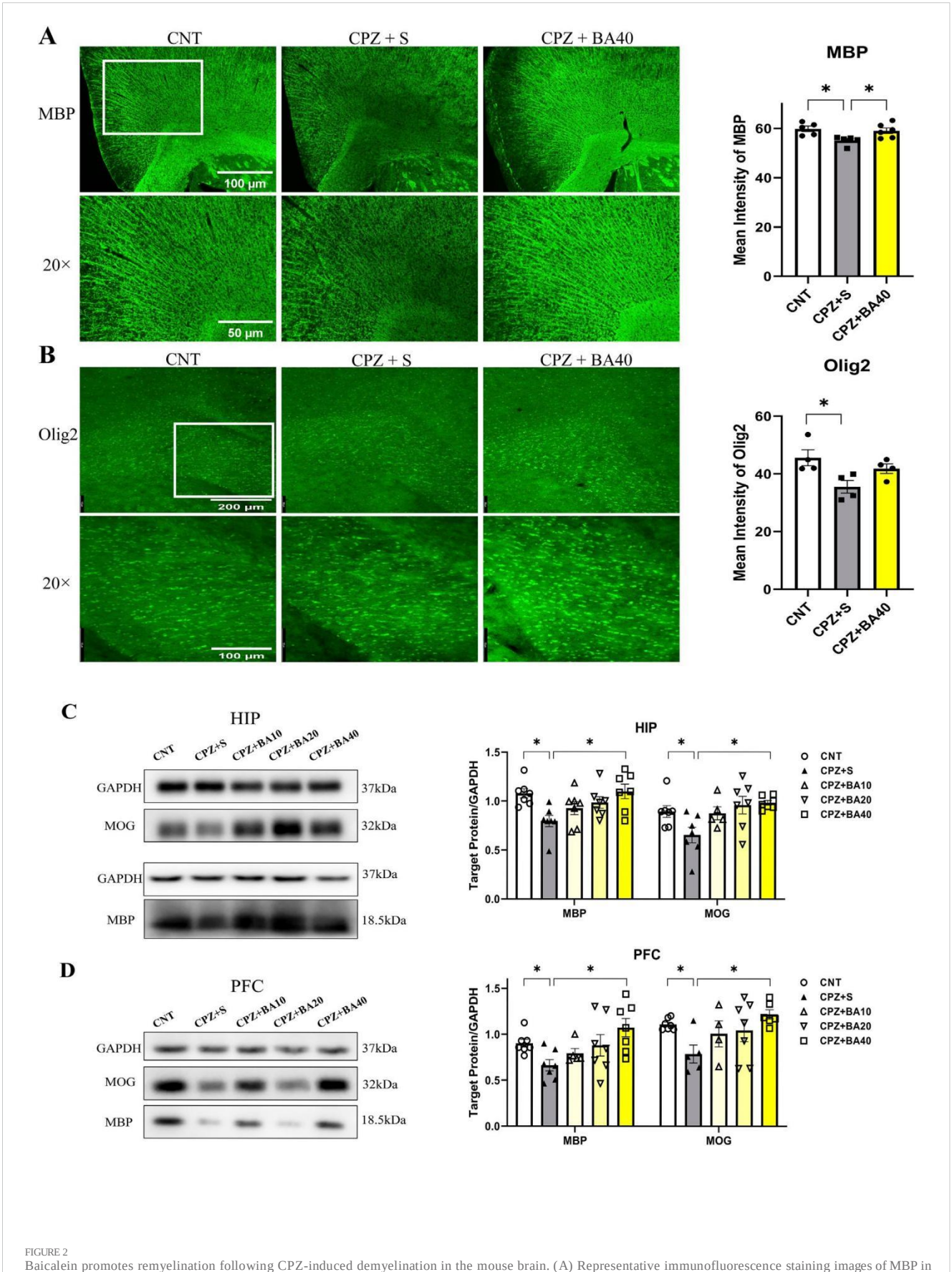

FIGURE 2
Baicalein promotes remyelination following CPZ-induced demyelination in the mouse brain. (A) Representative immunofluorescence staining images of MBP in the cerebral cortex and the statistical analysis of MBP MFI there (n = 5/group). (B) Representative immunofluorescence staining images of Olig2 in the corpus callosum and the statistical analysis of Olig2 MFI there (n = 4/group). (C) The representative Western blotting images of MBP and MOG proteins in HIP and the quantitative analysis of the proteins there (n = 5–7/group). (D) The representative Western blotting images of MBP and MOG proteins in the cerebral cortex and the quantitative analysis of the proteins there (n = 4–7/group). *$p < 0.05$, data are presented as mean ± SEM.

CPZ+S had a significant lower MFI of MBP relative to CNT group ($p = 0.0235$) or CPZ+BA40 group ($p = 0.0482$), there was no difference between CNT and CPZ+BA40 groups (p = ns). These results suggest that administration of BA at 40 mg/kg promoted the remyelination process in brains of mice following the CPZ-induced demyelination.

To provide further evidence for the above inference, we measured the MFI of oligodendrocyte transcription factor 2 (Olig2) IFS in the brains of mice from the same three groups. Figure 2B shows representative Olig2 IFS images taken at the corpus callosum (CC). Close observation of these images at a higher magnification tells obvious difference in Olig2 immunostaining in CC. Consistent with this visual observation, quantitative data of Olig2 MFI reported a significant effect of grouping ($F = 5.075$, $p = 0.0334$). Post-hoc comparisons showed a significant difference between CPZ+S and CNT groups ($p = 0.0285$), indicating an inhibiting effect of CPZ exposure on the development of OL lineage cells in this brain region. However, no difference was found between CNT and CPZ+BA40 groups (p = ns), suggesting a protective effect of BA (at the dose of 40 mg/kg) against the toxic effect of CPZ on OL lineage cells.

Further evidence came from the Western blotting analysis of MBP and myelin oligodendrocyte glycoprotein (MOG) in HIP and PFC of mice from all five animal groups. Figure 2C presents the representative Western blotting images of MBP and MOG (GADPH as the internal control), plus the quantitative data of the two proteins in HIP. One-way ANOVA revealed a significant effect of grouping on MBP ($F = 4.006$, $p = 0.0101$) and MOG ($F = 3.830$, $p = 0.0132$) expression levels. Post-hoc comparisons reported significant lower levels of MBP and MOG in the CPZ+S group relative to the CNT group ($p = 0.0223$, $p = 0.0334$, respectively) and to the CPZ+BA40 group ($p = 0.0121$, $p = 0.0128$, respectively). There was no significant difference between CNT group and any one of BA-treated groups. Similar changes were also seen in the expression levels of MBP and MOG in PFC of the mice, i.e., there was a significant effect of grouping on MBP ($F = 3.428$, $p = 0.0211$) and MOG ($F = 2.863$, $p = 0.0452$) expression levels. MBP and MOG levels in the CPZ+S group were significantly lower compared to the CNT group ($p = 0.0101$, $p = 0.0252$, respectively) and CPZ+BA40 group ($p = 0.0075$, $p = 0.0037$, respectively). There was no significant difference between CNT group and any one of BA-treated groups (Figure 2D).

3.3 Baicalein suppressed neuroinflammation in cuprizone-exposed mice

We performed IFS on brain sections of mice in the three groups of CNT, CPZ+S, and CPZ+BA40 with the antibodies specific to GFAP and IBA1. Figure 3A shows the representative images of the $GFAP^+$ cells in HIP of the mice in these three groups. The $GFAP^+$ cells in the CPZ+S image seem to be more densely packed than those in the other two images from CNT and CPZ+BA40 groups, respectively. One-way ANOVA revealed a significant effect of grouping on the density of $GFAP^+$ cells in the CA3 region of HIP. Post-hoc multiple comparisons reported that the number of $GFAP^+$ cells in the CA3 region of the CPZ+S group was significantly higher compared to those in the CNT group ($p = 0.0175$) and those in the CPZ+BA40 group ($p = 0.0038$). Similar changes were also found in $IBA1^+$ cells. The $IBA1^+$ cells in the CPZ+S image seem to be more densely packed than those in the other two images from CNT and CPZ+BA40 groups, respectively (Figure 3B). One-way ANOVA revealed a significant effect of grouping on the density of $IBA1^+$ cells in the CA3 region of HIP. Post-hoc comparisons reported that the number of $IBA1^+$ cells in the CA3 region of the CPZ+S group was significantly higher compared to those in the CNT group ($p = 0.0112$) and those in the CPZ+BA40 group ($p = 0.0104$).

To provide further evidence for the aforementioned IFS findings, we assessed the expression levels of GFAP protein in the HIP and PFC of mice from all five groups ($n = 6$/group) by means of Western blotting. Figure 3C shows representative Western blotting images of GFAP protein expressed in HIP and PFC, plus the statistical analysis results of the Western blotting data. One-way ANOVA revealed a significant effect of grouping on GFAP expression levels in HIP ($F = 2.972$, $P < 0.05$). Post-hoc tests reported that the GFAP expression level in the CPZ+S group was significantly higher than that in the CNT group. There was no significant difference between any other two groups. For GFAP expression level in PFC, one-way ANOVA showed no significant effect of grouping on this measurement ($F = 1.540$, $p = 0.235$).

The proliferation and activation of microglia and/or astrocytes are always accompanied by changes in levels of inflammatory cytokines in the brain. Therefore, we quantitatively assessed the protein levels of pro-inflammatory cytokines (IL-6, TNF-α) and anti-inflammatory cytokines (IL-10, TGF-β) in the PFC and HIP regions of mice from each of the five animal groups. The results are presented in Figure 4. In PFC, one-way ANOVA showed significant effects of grouping on IL-6 ($F = 10.170$, $p < 0.0001$) and TNF-α ($F = 12.840$, $p < 0.0001$) levels. Post-hoc tests reported that IL-6 and TNF-α levels in the CPZ+S group were significantly higher than those in the CNT group ($p < 0.0001$ in both comparisons). The levels of these two cytokines were also significantly higher relative to those in CPZ+BA40 group ($p = 0.0014$, $p = 0.0002$, respectively). There was no difference between any other two groups in levels of these two inflammatory cytokines. As for IL-10 in PFC, one-way ANOVA showed a significant effect of grouping on this measure ($F = 5.917$, $p = 0.0017$). Post-hoc tests reported that IL-10 level in the CPZ+S group was significantly lower than that in the CNT group ($p = 0.0032$). There was no difference between the other any two groups in this index. Also, one-way ANOVA showed a significant effect of

grouping on TGF-β level (F = 8.764, p = 0.0001) in PFC. Post-hoc tests reported that TGF-β level in the CPZ+S group was significantly higher than those in the CNT and CPZ+BA40 groups (p < 0.0001, p = 0.0095, respectively). There was no difference between the other any two groups in this measure (Figure 4A).

Similar changes in these inflammatory cytokines happened in the HIP region. One-way ANOVA showed significant effects of grouping on IL-6 (F = 17.370, p < 0.0001) and TNF-α (F = 11.070,
p < 0.0001) levels. Post-hoc tests reported that IL-6 and TNF-α levels
in the CPZ+S group were significantly higher than those in the CNT group (p < 0.0001 in both comparisons). The levels of these two cytokines were also significantly higher relative to those in CPZ+BA40 group (p < 0.001 in both comparisons). There was no difference between the other any two groups in levels of these two inflammatory cytokines. As for IL-10 in HIP, one-way ANOVA showed a significant effect of grouping on this measure (F = 20.750,

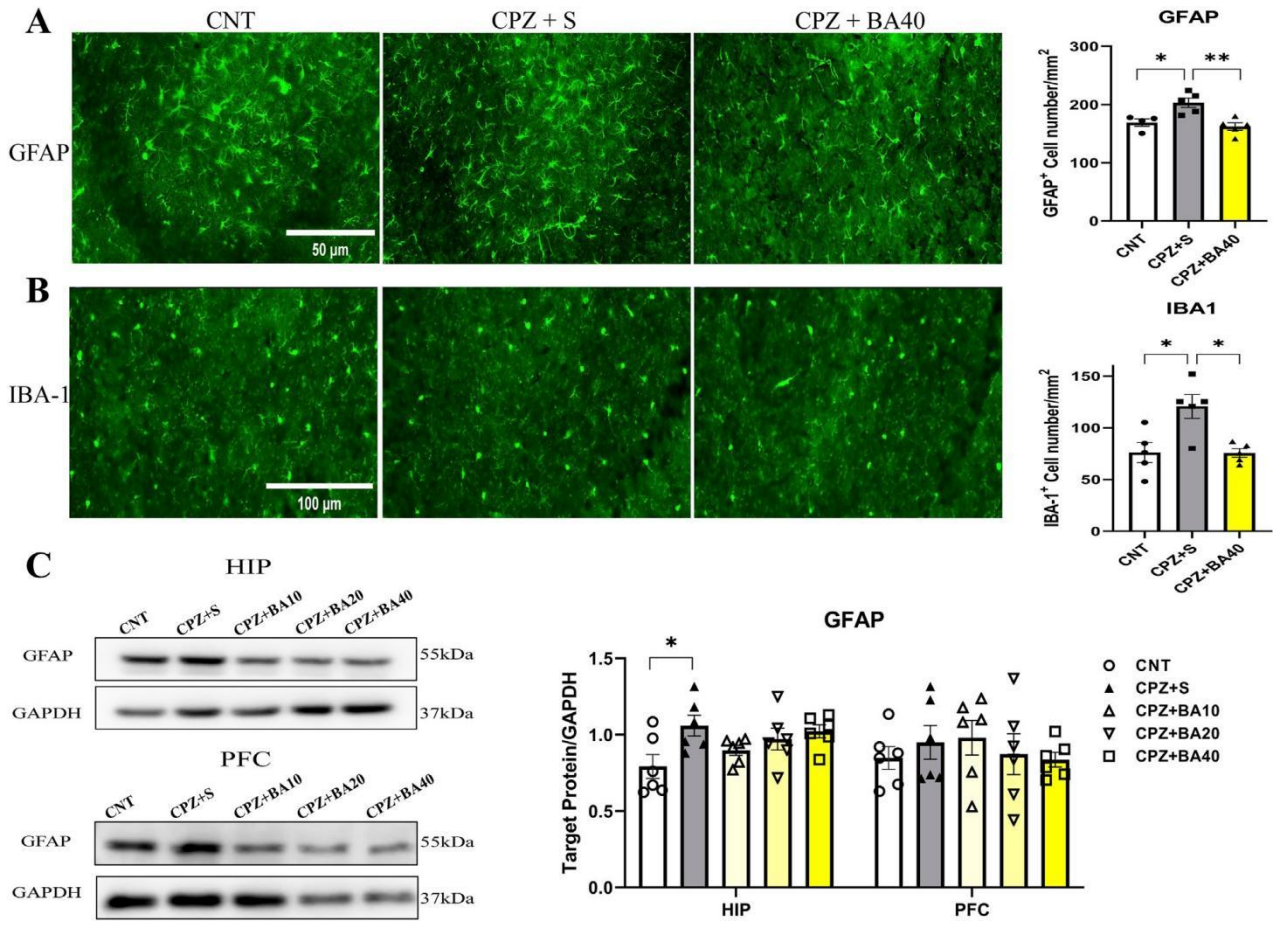

FIGURE 3
Baicalein alleviates the CPZ-induced proliferation of astrocytes and microglia in the mouse brain. (A) Representative immunofluorescence staining images of GFAP in the CA3 region of HIP and statistical analysis of GFAP⁺ cell density there (n = 5/group). (B) Representative immunofluorescence staining images of IBA-1⁺ cells in the CA3 region and statistical analysis of IBA-1⁺ cell density there (n = 5/group). (C) Representative Western blotting images of GFAP in the HIP and PFC and statistical analysis of GFAP expression in the brain regions (n = 6/group). *$p < 0.05$, data are presented as mean ± SEM.

$p < 0.0001$). Post-hoc tests reported that IL-10 level in the CPZ+S group was significantly lower than those in the CNT and CPZ+BA40 groups ($p < 0.001$ in both comparisons). There was no difference between the other any two groups in this index. Also, one-way ANOVA showed a significant effect of grouping on TGF-β level ($F = 9.655$, $p < 0.0001$) in HIP. Post-hoc tests reported that TGF-β level in CNT group was the highest among the five groups. There was no difference among the other four groups in this measure (Figure 4B).

3.4 Baicalein improved mitochondrial dysfunction in CPZ-exposed mice

Previous studies have shown that CPZ impairs mitochondrial function of neural cells thereby causing demyelination in CNS of mice (Faizi et al., 2016; Luo et al., 2020). We expected that baicalein might protect brain cells against the toxic effects of CPZ on mitochondrial function in mice. To test this hypothesis, we assessed mitochondrial function of neural cells in HIP of all mice in this study by means of Western blotting. Figure 5A shows representative Western blotting images of mitochondrial respiratory chain complexes CII-CV of neural cells of mice from each group (CI was not shown). The quantitative data of all images were presented in Figure 5A (right). One-way ANOVA revealed significant effects of grouping on protein levels of CIV ($F = 5.461$, $p = 0.0031$) and CV ($F = 4.190$, $p = 0.004$). The grouping effect was at a marginal level on CII ($p = 0.058$). Post-hoc comparisons reported that CII level in CPZ S group was significantly lower compared to the CNT group ($p = 0.0234$), there was no difference between CNT and CPZ+BA40 groups (p = ns). The CIV and CV levels in CPZ+S group were significantly lower than those in CNT ($p = 0.0394$, $p = 0.041$, respectively) and CPZ+BA40 groups ($p = 0.0181$, $p = 0.0458$, respectively).

Furthermore, we assessed the protein levels of NAT8L (aspartate N-acetyltrasferase) in HIP and PFC of mice in the four groups (CPZ+BA10 was not included). NAT8L is a mitochondrial protein that catalyzes the synthesis of N-acetylaspartate (NAA) from aspartate and acetyl-CoA in mitochondria of neuron. The representative Western blotting images of NAT8L in HIP and PFC of mice were presented on the upper and lower rows of the left panel of Figure 5B, respectively, while the statistical analysis of

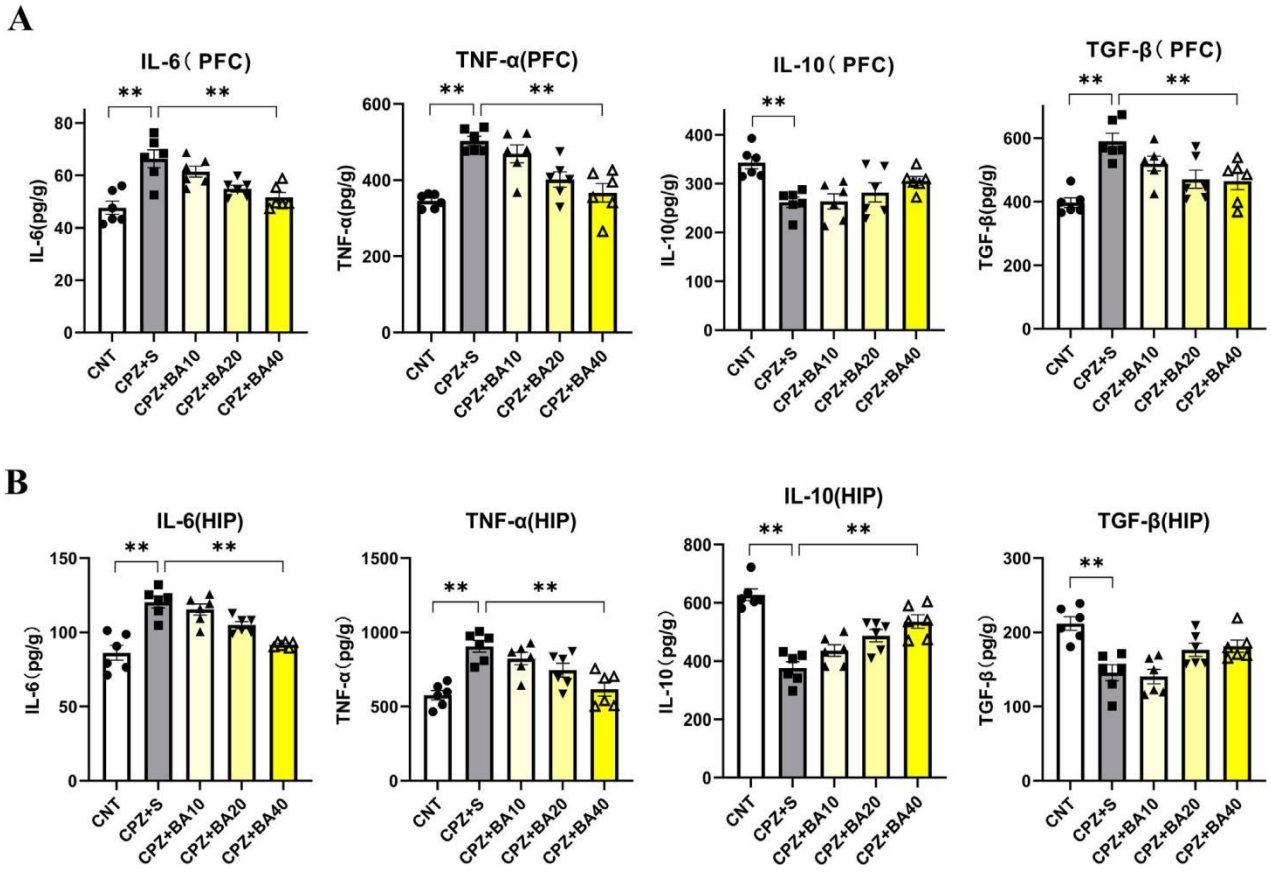

FIGURE 4
Baicalein reverses the CPZ-induced changes in levels of inflammatory cytokines in the mouse brain. (A) Bar charts showing the levels of IL-6, TNF-α, IL-10 and TGF-β in the PFC (n = 6/group). (B) Bar charts showing the levels of IL-6, TNF-α, IL-10 and TGF-β in the HIP (n = 6/group). *$p < 0.05$, **$p < 0.01$. Data are presented as mean ± SEM.

the protein levels in the two brain regions of mice is shown in the right panel of this figure. One-way ANOVA revealed a significant effect of grouping on NAT8L levels in HIP ($F = 4.956$, $p = 0.0183$), but not on that in PFC ($F = 0.38$, p = ns). Post-hoc comparisons reported that NAT8L level in HIP of mice from the CPZ+S group was significantly lower than those in the CNT and CPZ+BA40 groups ($p = 0.0433$, $p = 0.0468$, respectively).

3.5 Baicalein regulated the NRF2 redox pathway in CPZ-exposed mice

Oxidative stress and mitochondrial dysfunction in MS (Kim et al., 2015) are partly attributed to the imbalance of the NRF2 signaling pathway, which regulates redox homeostasis and mitochondrial function and plays a crucial role in modulating neuroinflammation (Branca et al., 2017; Brandes and Gray, 2020; Chen et al., 2009; MichaliČKovÁ et al., 2020). To explore the mechanism underlying the beneficial effects of BA on remyelination following CPZ-induced demyelination in mice, we measured the expression levels of NRF2 and its downstream targets (HO-1, NQO1, and SOD2) in the HIP of mice by means of ELISA. The results are presented in Figure 6. One-way ANOVA revealed a significant effect of grouping on NRF2 levels ($F = 17.080$, $p <$ 0.0001). Post-hoc comparisons reported that NRF2 level in CPZ+S group was significantly higher than those in CNT and CPZ+BA40 groups ($p < 0.0001$ in both comparisons) (Figure 6A). The same changes are also seen in levels of HO-1, SOD2, and NQO1. That is, levels of these downstream molecules of the NRF2 signaling pathway in CPZ+S group are significantly higher than those in CNT and CPZ+BA40 groups (Figures 6B–D, respectively).

3.6 Baicalein protected against the inhibitory effects of CPZ on the development of OL lineage cells

To provide further evidence that BA protects against inhibitory effects of CPZ on the development of OL lineage cells, we did *in vitro* experiments with cultured OLs. During the OPC proliferation phase (DIV11-12), we treated the cells with various concentrations of CPZ (0, 0.025, 0.05, 0.1, 0.5, 1.0, 2.0 mM) for 24 h and measured OPCs viability using the CCK8 assay kit. The quantitative results are shown in Figure 7A. One-way ANOVA revealed a significant main effect of CPZ on OPCs viability ($F = 62.920$, $p < 0.0001$). Post-hoc comparisons reported that CPZ dose-dependently reduced OPCs viability as compared to the CNT group. Based on these

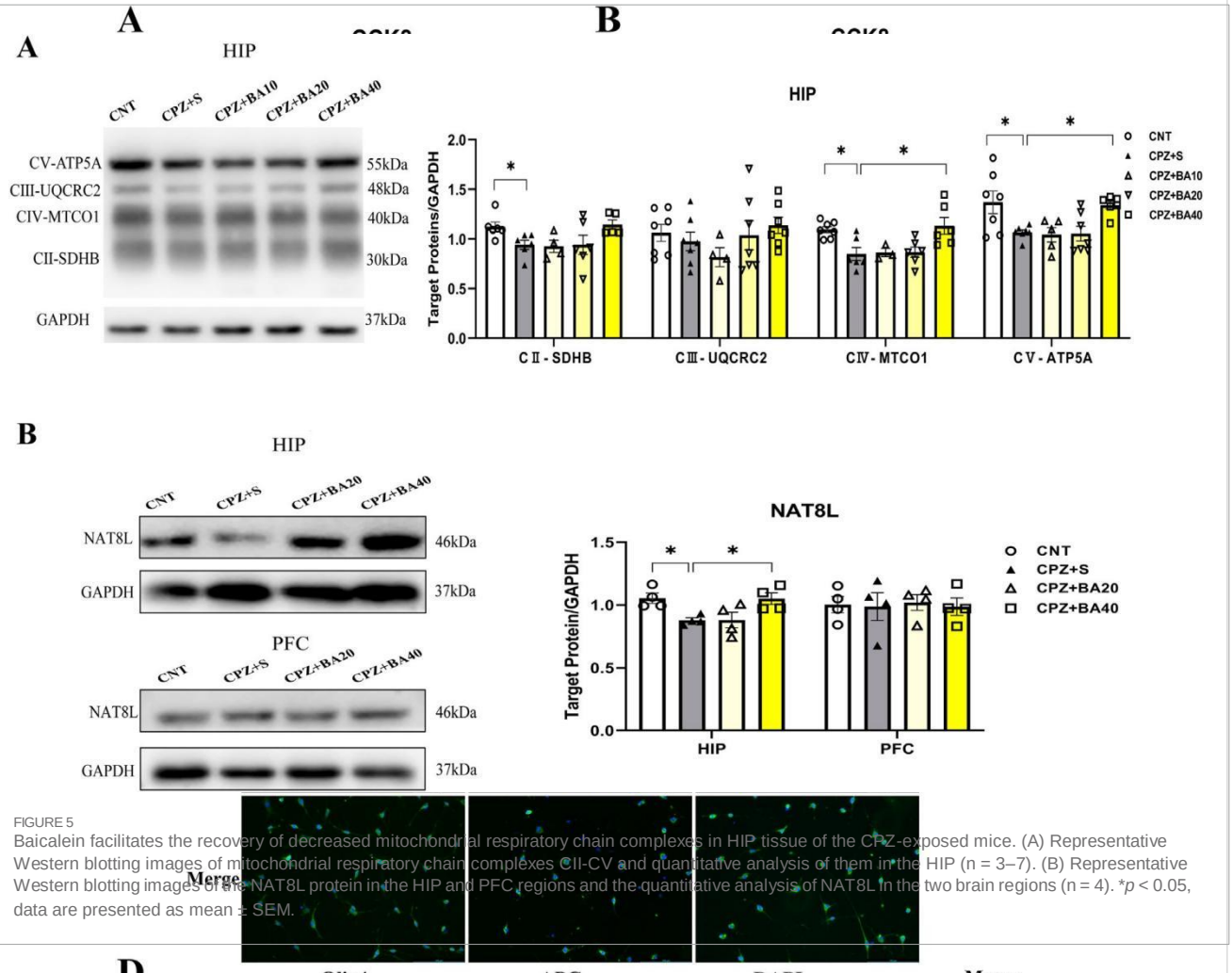

FIGURE 5
Baicalein facilitates the recovery of decreased mitochondrial respiratory chain complexes in HIP tissue of the CPZ-exposed mice. (A) Representative Western blotting images of mitochondrial respiratory chain complexes CII-CV and quantitative analysis of them in the HIP (n = 3–7). (B) Representative Western blotting images of the NAT8L protein in the HIP and PFC regions and the quantitative analysis of NAT8L in the two brain regions (n = 4). *$p < 0.05$, data are presented as mean ± SEM.

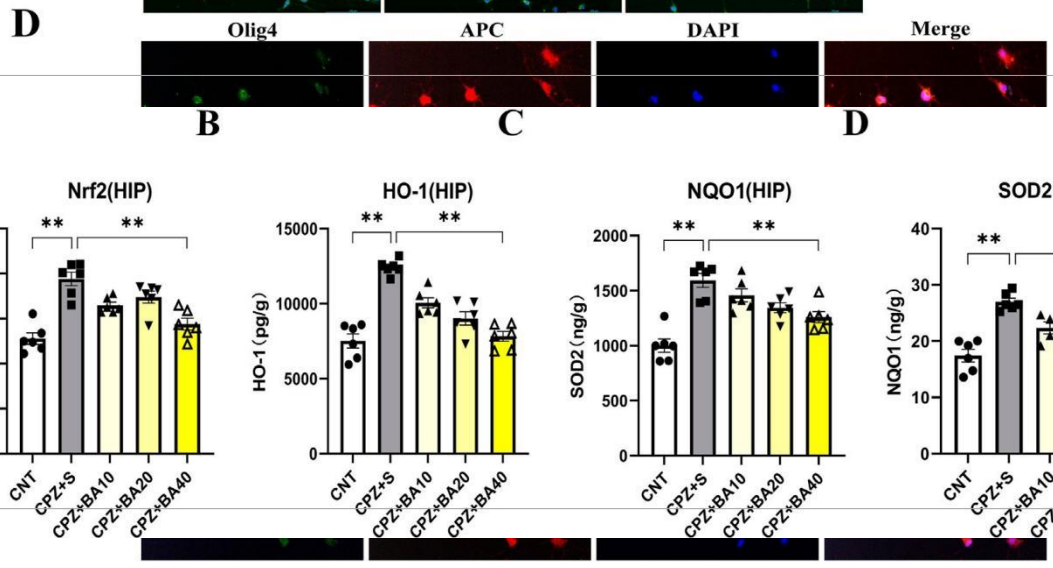

FIGURE 7
Baicalein blocks the inhibitory effects of CPZ on the viability and development of cultured OL lineage cells. (A) CPZ decreases the viability of cultured OPCs in a dose-dependent manner, n = 3/group. (B) BA (40 μM) blocks the inhibitory effect of CPZ on the viability of cultured OPCs, n = 3/group. (C) Representative immunofluorescence staining images of $Olig2^+$ cells cultured under the indicated conditions. (D) Representative immunofluorescence staining images of the cells expressing both APC (red) and Olig4 under the indicated conditions. The cell nuclei were labeled by DAPI (blue). $*p < 0.05$, $**p < 0.01$. Data are presented as mean ± SEM.

results, 0.5 mM CPZ and 20 μM BA were chosen to examine possible protective effect of BA on the inhibitory effect of CPZ on OPC proliferation and cell viability. The cells (on DIV11-12) were cultured in three different conditions, i.e., in the absence of CPZ and BA (CNT), in the presence of CPZ (0.5 mM), and in the presence of BA (20 μM) and CPZ (0.5 mM). The results showed a significant main effect of treatment on cell viability ($F = 13.300$, $p = 0.0062$). Post-hoc comparisons reported that CPZ-treated cells had significantly lower viability than the CNT ($p = 0.0058$) and CPZ+BA ($p = 0.0276$) groups (Figure 7B). In line with the CCK8 assay results, IFS of the cultured cells showed that CPZ group have fewer $Olig2^+$ cells relative to the other two groups (see the images on the first row of Figure 7C). And there were many more DAPI-stained nuclei that were smaller (on the second row of Figure 7C) and not overlapped with green-stained cell body and processes (third row of Figure 7C), indicative of condensed nuclei of the dying cells. These results suggest that BA attenuates the inhibitory effects of CPZ on OPCs proliferation and activity.

With the same treatments, another batch of cell cultures started on DIV13 and lasted for 24 h. Then the cultured cells were subjected to IFS with the antibody against $Olig4^+$ (a biomarker of immature OLs) or APC^+ (a biomarker of mature OLs). As shown in Figure 7D, some of the DAPI-stained nuclei on the second row look smaller relative to the others on the first and third rows. In the fourth column with cell images from the superposition of $Olig4^+$ and APC^+, some cell profiles appear pure green in the CPZ (0.5 mM) group, indicating that these immature OLs did not develop to mature ones in the presence of CPZ. This phenomenon was not seen in CNT and CPZ+BA20 groups, indicating that BA attenuated the inhibitory effects of CPZ on the maturation of immature OLs.

3.7 Baicalein protected cultured OLs and OLN-93 cells against the toxic effects of CPZ on mitochondria of the cells

To provide further evidence for the protective effects of baicalein on mitochondrial function of the cultured OLs, we evaluated the mitochondrial membrane potential of OLs cultured under various conditions [in the absence of CPZ and BA, in the presence of CPZ (0.5 mM), or in the presence of CPZ (0.5 mM) + BA (40 μM)]. The culturing lasted for 24 h followed by the assessment of mitochondrial membrane potential of the cultured OLs on DIV13 using the JC-1 kit. As shown in Figure 8A, the CPZ- treated cells appear lighter red fluorescence, but darker green fluorescence, relative to those in the CNT and CPZ+BA groups, indicating the presence of mitochondrial membrane damage in the CPZ-treated cells, which was blocked by BA at the concentration of 40 μM.

Moreover, we did another experiment with the OLN-93 cell line (an immortalized OL cell line) treated with various concentrations of H_2O_2 (0, 0.2, 0.4, 0.8, 1.6 mM) for 24 h, followed by cell viability assessment by means of the CCK8 assay. The quantitative results are presented in Figure 8B. One-way ANOVA revealed a significant main effect of H_2O_2 concentration on OLN-93 viability (% of CNT). Compared to the CNT group, H_2O_2 dose-dependently reduced cell viability of OLN-93. Based on these results, the OLN-93 cell line were cultured in another experiment in the presence of 400 μM H_2O_2, 400 μM H_2O_2 plus 40 μM BA, or in the absence of H_2O_2 and BA (Control). The culture maintained for 24 h. Then cell viability and ROS levels in the cultures were measured. As shown in Figure 8C, the main effect of treatment on cell viability was significant ($F = 5.610$, $p = 0.0423$). Post-hoc comparisons reported a significant difference between CNT and H_2O_2 (400 μM) groups. As for ROS levels, OLN-93 cells treated with H_2O_2 (400 μM) showed strongest green fluorescence relative to those in the other two groups (Figure 8D). These differences were confirmed by the quantitative analysis of the fluorescence intensity of cultured cells in the three groups (Figure 8E). One-way ANOVA revealed a significant effect of grouping on integrated density of the fluorescence staining of cultured cells ($F = 11.510$, $p = 0.0088$). Post- hoc comparisons reported the highest level of fluorescence intensity in the H_2O_2 group relative to the CNT ($p = 0.0083$) and the 400 μM H_2O_2+40 μM BA ($p = 0.0372$) groups.

4 Discussion

Demyelination, OL apoptosis, and astrocyte and microglia activation are hallmarks of MS pathophysiology, which culminates in unsuccessful remyelination (Podbielska et al., 2013; van der Valk and De Groot, 2000). The hallmark impairments of multiple sclerosis are caused by demyelination, which disrupts axonal conduction (Sriram, 2011). Thus, boosting remyelination and decreasing demyelination are important approaches to treating multiple sclerosis (MS) (Dolati et al., 2017). Many traditional Chinese medicines are being researched more and more as complementary and alternative therapies in the quest for new medications to treat multiple sclerosis. Because of its anti-inflammatory, antioxidant, and cognitive-enhancing qualities, BA was thoroughly examined in the current study with regard to its effects on CPZ-

induced neuropathological changes and behavioral abnormalities in the CPZ-exposed mice (Brinza et al., 2021; Gregory et al., 2021; Shi et al., 2023). The three hydroxyl groups (at positions 5, 6, and 7) in BA's structure (Supplementary Figure 1) are partially responsible for its potent antioxidant qualities. By oxidizing these groups, the molecule may scavenge ROS (de Oliveira et al., 2015). Furthermore, BA has the ability to produce persistent semiquinone radicals, which support its strong antioxidant properties (Gao et al., 1999).

In line with other research conducted by our team and others (Mihai et al., 2021; Yang et al., 2020a; Zhang et al., 2017), the mice in our investigation that were exposed to CPZ showed demyelination in the cerebral cortex, HIP, and CC. Additionally, these mice had reduced spontaneous alternation rates in the Y-maze test, a considerably shorter initial flip delay in the rotarod test, and a lower RI in the NOR test retention trials. These behavioral anomalies in CPZ-exposed mice point to the existence of compromised motor coordination and cognitive function brought on by CPZ exposure, which is similar to the above-mentioned clinical signs seen in MS patients. Crucially, BA treatment for two weeks after four weeks of CPZ exposure markedly improved the previously mentioned abnormalities in brain function while promoting the remyelination process, as shown by higher MBP and Olig2 IFS as well as higher levels of MBP and MOG in the PFC and HIP of mice exposed to CPZ. When considered together, it is conceivable that BA encouraged remyelination.

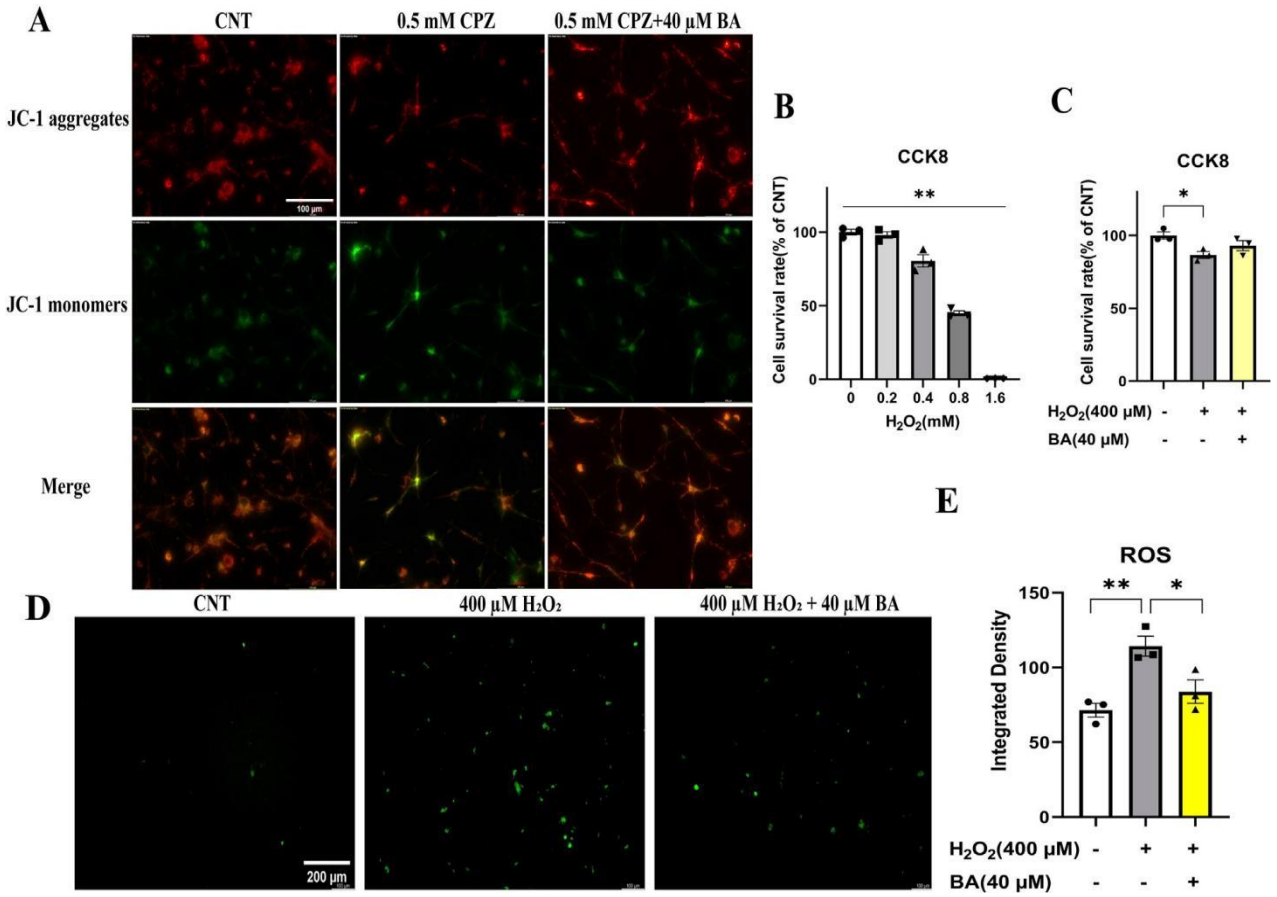

FIGURE 8
Baicalein prevents cultured OLs from the CPZ-induced mitochondrial membrane potential decrease and blocks the inhibitory effect of H_2O_2 on viability of OLN-93 cells by decreasing the production of ROS in the H_2O_2-treated cells. (A) BA prevents cultured OLs from the CPZ-induced mitochondrial membrane potential decrease. (B) H_2O_2 decreases the viability of OLN-93 cells in a dose-dependent manner. (C) BA prevents OLN-93 cells from H_2O_2-induced viability decrease. (D) Representative ROS fluorescence images of OLN-93 cells cultured under the indicated conditions, n = 3/group. (E) Quantitative analysis of ROS fluorescence intensity in OLN-93 cells cultured under the indicated conditions. *$p < 0.05$, **$p < 0.01$. Data are presented as mean ± SEM.

in the brain of CPZ-exposed mouse thereby improving motor and cognitive deficits in the animals. This conclusion aligns with the commonly accepted notion that it is demyelination in both white and gray matter in the brain that lead to motor dysfunction and cognitive impairments such as attention deficits and long-term memory loss (Calabrese et al., 2011; Franco-Pons et al., 2007; Hibbits et al., 2009; Kutzelnigg et al., 2005; Woo et al., 2024).

MS patients exhibit pathological features of inflammatory infiltration and glial cell proliferation. Relevantly, the CPZ- induced mice present astrocyte and microglial proliferation and activation, along with increased levels of inflammatory cytokines such as TNF-α and IL-1β. These inflammatory factors act synergistically and impair mitochondrial function of OLs and increase ROS levels as shown in previous studies (Abdel-Maged et al., 2020; Arnett et al., 2001; Pasquini et al., 2006). ROS, in turn, damage mitochondria by blocking complexes in the respiratory chain, leading to OLs apoptosis and ultimately demyelination (Kipp et al., 2009; Mahad et al., 2008; Praet et al., 2014). In consistent with these previous studies, the present study found that CPZ-exposed mice had significantly increased numbers of $GFAP^+$ and $IBA1^+$ cells in the cerebral cortex and HIP, along with elevated GFAP in HIP, suggesting the presence of neuroinflammation in brain tissue of the CPZ-exposed mice. Further supporting evidence for this inference, the CPZ-exposed mice in this study showed higher levels of pro-inflammatory cytokines TNF-α and IL-6, but significantly lower levels of anti-inflammatory cytokines IL-10 and TGF-β. However, BA given at 40 mg/kg/day for 2 weeks following CPZ-exposure for 4 weeks alleviated the CPZ-induced neuroinflammation, while promoting the remyelination process as discussed above. The concurrent anti-inflammation and promyelinating effects of BA (40 mg/kg/gay for 2 weeks) added further evidence for the application of anti-inflammation drugs in patients with MS. It also highlights the complex interplay between inflammation and demyelination in CNS (Ganz et al., 2023; Zveik et al., 2022; Zveik et al., 2024).

The initial effect of CPZ on neural cells lies in its toxicity to the cells' mitochondria. Therefore, we examined possible effects of BA on mitochondria of brain cells in CPZ-exposed mice. We found that protein levels of mitochondrial respiratory complexes II, IV, and V (ATP synthase) were significantly lower in the HIP of CPZ-treated mice, along with decreased levels of NAT8L, a marker of neuronal mitochondrial function, indicating the damaging effect of CPZ on mitochondria of both neurons and glia cells. Moreover, BA40 effectively reversed these mitochondria function impairments induced by CPZ-exposure. Further evidence for the damaging effects of CPZ on mitochondrial function of brain cells came from the analysis of the NRF2 pathway, which is a crucial defense mechanism of the cellular response to oxidative stress and mitochondrial dysfunction. The CPZ exposure significantly elevated levels of NRF2 and its down-stream antioxidant enzymes of HO-1, NQO1, and SOD2, confirming the upregulation of this pathway in response to the oxidative stress induced by CPZ exposure. More importantly, BA intervention restored the upregulation of these pathway proteins to normal levels in a dose-dependent manner, suggesting that BA protects the NRF2 pathway from over-activation, maintaining it at normal levels through its antioxidant effects. Certainly, these findings have broad relevance to clinical research advances in MS pathogenesis and treatment. For example, MS patients exhibited mitochondrial dysfunctionand impaired mitochondrial respiratory chain complexes, leading to axonal degeneration and demyelination (Campbell and Mahad, 2012; Dutta et al., 2006; Komiyama et al., 2022; Maldonado et al., 2022). Abnormally activated NRF2 pathway was also reported in MS patients (Dinkova-Kostova and Abramov, 2015; Draheim et al., 2016; Licht-Mayer et al., 2015; Rosito et al., 2020). Moreover, the therapeutic effects of the clinical MS drug dimethyl fumarate are believed to be related to this pathway (Uruno and Yamamoto, 2023; Yan et al., 2021).

To provide further evidence for the toxic effects of CPZ on the survival and development of OL lineage cells and the protective effects of BA on these cells, we did *in vitro* experiments with OL lineage cells and OLN-93 cell line. It was found that CPZ dose- dependently decreased the viability of cultured OLs during the OPC proliferation phase (DIV11-12), but this toxic effect was not seen in cultured cells in the presence of BA (20 μM) and CPZ (0.5 mM). This set of data added evidence for the protective effect of BA on OPCs survival and growth in the *in vitro* microenvironment lacking microglia and astrocytes. Going further, we found that CPZ (0.5 mM) suppressed the development of $Olig4^+$ cells into more mature APC^+ cells. And these inhibitory effects were effectively blocked in the CPZ+BA group. In later stages of OL development, CPZ-exposure inhibited the maturation of OLs as some cells stayed at the immature stage ($Olig4^+$ cells), but these immature OLs were not seen in the CNT and CPZ+BA groups. Taken together, CPZ suppressed the development of cultured OL lineage cells in the inflammation-free environment, but BA prevented the cultured OL lineage cells from this inhibition of CPZ, thereby allowing the normal growth and development of cultured OL lineage cells.

Last but not least, JC-1 assays revealed that mitochondrial membrane potential of cultured OLs was significantly lower in the CPZ-treated cells compared to the CNT group, but BA (20 μM) blocked this effect. These data added direct evidence that both CPZ and BA impact on mitochondria of cultured OLs in damaging and protecting manners, respectively. Further evidence for the protective effect of BA on mitochondria of cultured OLs

came from the experiment with OLN-93 cells treated with various concentrations of H_2O_2 in the absence or presence of BA. CCK8 assays reported that H_2O_2 dose-dependently reduced the viability of OLN-93 cells, but BA (40 μM) completely blocked this effect. The H_2O_2 (400 μM) treatment significantly increased ROS level in the culture medium, but this effect was completely blocked in OLN-93 cells treated H_2O_2 and BA (40 μM). Consistent with our results, the H_2O_2-induced oxidative stress was reported in a recent study with cultured OLN-93 cells (Li F. et al., 2021). BA has been shown to scavenge free radicals and reduce ROS production in various cell types (Gao et al., 1999; Saija et al., 1995), protect the cells against oxidative damage (Jeong et al., 2019; Ma et al., 2018; Park et al., 2019). All the BA doses used in animal and cell culture experiments in present study are comparable to that used in previous human studies in which 100–2,800 mg/day BA were given to healthy Chinese, showing no significant side effect in the subjects. Therefore, the data from the present study encourage the translational application of BA in clinical practice for MS patients (Dong et al., 2021; Li et al., 2014).

5 Conclusion

In conclusion, our in vivo studies showed that BA promotes the remyelination process and reduces neuroinflammation in the brains of CPZ-exposed mice, hence aiding in the recovery of motor dysfunction and cognitive deficits. BA intervention keeps the signal pathway at comparatively normal levels by preventing the NRF2 pathway from over-activating in response to CPZ exposure, which underlies these protective benefits. Both CPZ and H2O2 slow down the development of the cultivated OL lineage cells by destroying their mitochondria, however BA successfully stops the development delay of the cultured OLs by scavenging ROS that are generated by the cells' damaged mitochondria. These collections of in vitro and in vivo data support the therapeutic use of BA in the treatment of MS patients in the future.

References

Awad, A. S., Mohamed, E. A., Azab, S. S., Rashed, L. A., Gad, A. M., and Abdel-Maged, A. E. S. (2020). Using secukinumab as a neuroprotective agent by inhibiting oxidative, inflammatory, and neurodegenerative signals in an animal model of multiple sclerosis produced by cuprizone. Mol. neurobiology. 57, 3291–3306. 10.1007/s12035-020-01972-9 is the doi

Mason, J., Suzuki, K., Matsushima, G. K., Arnett, H. A., Marino, M., and Ting, J. P. Y. (2001). TNFα stimulates remyelination and the growth of oligodendrocyte progenitors. Nat. Neurosci. 4, 1116–1122. 10.1038/nn738

Chinnery, P. F., and Bargiela, D. (2019). Mitochondria in neuroinflammation: Leber Hereditary Optic Neuropathy (LHON), Multiple Sclerosis (MS), and LHON-MS. Neurosci. Let's. 132932, 710. 10.1016/j.neulet.2017.06.051 is the doi.

Inglese, M. and Bermel, R. F. (2012). The eye tells us about the storm: inflammation and neurodegeneration in multiple sclerosis. 20–19 in Neurology 80. 10.1212/WNL is the doi. 0b013e31827b1b6c

Nguyen, T.-V., Doyle, K., Branca, C., Ferreira, E., Caccamo, A., and Oddo, S. (2017). In a mouse model of Alzheimer's disease, cognitive deficiencies are made worse by genetic Nrf2 decrease. Hmm. Mol. Genet. 26, 4823–4835. 10.1093/hmg/ddx361 is the doi

Gray, N. E., and Brandes, M. S. (2020). A potential treatment target for neurodegenerative disorders is NRF2. ASN Neuro 12, 1419899782, 1759092. The reference is 10.1177/1759091419899782.

Brinza, I., Eldahshan, O. A., Hritcu, L., and Ayoub, I. M. (2021). Through the regulation of cholinergic and antioxidant systems, baicalein 5,6-dimethyl ether protects memory impairments in the scopolamine zebrafish model. Plants 10, 1245. 10.3390/ plants10061245 is the doi.

Gallo, P., Grossi, P., Rinaldi, F., and Calabrese, M. (2011). Multiple sclerosis-related cortical damage and cognitive impairment. Rev. Neurother, expert. 11, 425–432. doi:10. ERN.10.155/1586

Mahad, D. J., and Campbell, G. R. (2012). Demyelination-related mitochondrial alterations: implications for axonal integrity. 173–179 in Mitochondrion 12. doi:10. J. Mito.2011.03.007 1016

Chen, P. C., Johnson, D. A., Kan, Y. W., Pani, A. K., Smeyne, R. J., Vargas, M. R., et al. (2009). The astrocyte plays a crucial function in Nrf2-mediated neuroprotection in the MPTP mouse model of Parkinson's disease. Proc. National. Acad. Science. U. S. A. 106, 2933–2938. 10.1073/pnas.0813361106 is

the doi.

Comi, G., Hartung, H. P., Khatri, B. O., Montalban, X., Barkhof, F., Cohen, J. A., et al. (2010). Intramuscular interferon or oral fingolimod for relapse multiple sclerosis. N. English. 402–415 in J. Med. 362 (5). 1056/NEJMoa0907839 is the doi.

A. Corthay. (2006). A three-cell model for naïve T helper cell activation. Scand.

Immunol. J. 64, 93–96. 10.1111/j.1365-3083.2006.01782.x is the doi.

Carrì, M. T., Cozzolino, M., and D'Ambrosi, N. (2018). The function of redox (dys)regulation in neuroinflammation in amyotrophic lateral sclerosis. antioxidant. signal of redox. 29, 15–36. 10.1089/ars.2017.7271 is the doi

Nabavi, S. F., Habtemariam, S., Erdogan Orhan, I., de Oliveira, M. R., Daglia, M., and Nabavi, S. M. (2015). A review of baicalein's and baicalin's effects on mitochondrial dynamics and function. Pharmacol. Res. 100, 296–308. 1016/j.phrs.2015.08.021 is the doi.

Abramov, A. Y., and Dinkova-Kostova, A. T. (2015). Nrf2's newly discovered function in mitochondria. Radic Free. Biol. Med. 88, 179–188. 10.1016/j is the doi. 4.036 in freeradbiomed.2015.

Dolati, S., Sadreddini, S., Babaloo, Z., Jadidi-Niaragh, F., Ayromlou, H., and Yousefi,

M. (2017). Therapeutic uses of developing drug delivery technologies for multiple sclerosis. Biomed. pharmacist. 86, 343–353. Journal of Biopha.2016.12.010 doi:10.1016

Lou, K., Luo, H. M., Hao, S., Li, L. J., Gao, H. Z., Dong, R. H., et al. (2021). A single-center, randomized, double-blind, placebo-controlled, single-dose phase I trial was conducted to examine the safety, tolerability, pharmacokinetics, and food impact of baicalein tablets in healthy Chinese participants. J. ethnopharmacology. 114052, 274. 10.1016/j.jep.2021.114052 is the doi.

Scheld, M., Liessem, A., Draheim, T., Denecke, B., Wilms, F., and Weißflog, M. (2016). In an animal model of multiple sclerosis, activation of the astrocytic Nrf2/ARE system reduces the development of demyelinating lesions. 2219–2230 in Glia 64. doi:10. Glia.23058 1002/

Chang, A., Peterson, J., Dutta, R., McDonough, J., Yin, X., Torres, T., et al. (2006). Patients with multiple sclerosis may have axonal degeneration due to mitochondrial malfunction. Ann. Neurol. 59, 478–489. 10.1002/ana.20736 is the doi

Delacour, J. and Ennaceur, A. (1988). A novel one-trial test for neuroscience research on rat memory. 1. Data about behavior. Act. 47–59 in Brain Res. 31 (1). 10.1016/0166-4328(88)90157-x is the doi

Kouhnavard, M., Rahimi, A., Naserzadeh, P., Faizi, M., Salimi, A., Seydi, E., et al. (2016). Cuprizone, a Cu2+chelating agent, and its toxicity to the brain of a mouse

mitochondria: a rationale for demyelination and the behavioral impairment that follows.

poison. Mech. Techniques 26, 276–283. 10109/15376516.2016.1172284 is the doi.

Torrente, M., Vilella, E., Franco-Pons, N., and Colomina, M. T. (2007). behavioral abnormalities in the mouse model of demyelination/remyelination produced by cuprizone. poison. Let's. 169, 205–213. 1016/j.toxlet.2007.01.010 is the doi.

Stromsnes, K., and Gambini, J. (2022). From causes to treatment strategies, oxidative stress and inflammation are discussed. Biomedicines 10, 753. Biomedicines10040753 doi:10.3390

Ganz, T., Rechtman, A., Lachish, M., Zveik, O., Fainstein, N., Sofer, L., et al. (2023). Repair activities in the chronically demyelinated central nervous system are not supported by the differentiation stimulation of oligodendrocyte progenitor cells using MAPK/ERK inhibitors. 2815–2831 in Glia 71. 10.1002/glia.24453 is the doi.

Zhang, X. L., Gao, Z. H., Xu, H. B., and Huang, K. X. (1999). Flavonoids isolated from the radix of Scutellaria baicalensis georgi have antioxidant and free radical scavenging properties. Biochim. Biophys. Acta. 1472, 643–650. 10.1016/S0304-4165(99)00152-X is the doi

Yendluri, B. B., Blach-Olszewska, Z., Leszek, J., Parvathaneni, K., Gasiorowski, K., Lamer-Zarawska, E.,

et al. (2011). Scutellaria baicalensis georgi root flavones: potential future medications for neurodegeneration? Drug Targets for CNS and Neurological Disorders 10, 184–191. 10.2174/187152711794480384 is the doi.
Gregory, J., Bredesen, D. E., Rao, R. V., and Vengalasetti, Y. V. (2021). Herbs that protect neurons to treat Alzheimer's disease. Biomolecules 11,
543. For example, 10.3390/biom11040543
Iwasa, K., Yamashina, K., Ishikawa, M., Maruyama, K., Hashimoto, M., Yamamoto, S., et al. (2017). By inhibiting neuroinflammation, the flavonoid baicalein reduces the demyelination brought on by cuprizone. Brain Res. Bull. 135, 47–52. 10.1016/j is the doi. 9.007 Brainresbull.2017.
He, A., Trojano, M., Spelman, T., Jokubaitis, V., Havrdova, E., and Horakova, D. (2015). Comparing switching to interferon beta/glatiramer acetate or fingolimod in patients with active multiple sclerosis. JAMA Neurology. 72, 405–413. Jamaneurol.2014.4147 (doi:10.1001)
Armstrong, R. C., Wu, T. J., Hibbits, N., and Pannu, R. (2009). In mice, cuprizone demyelination of the corpus callosum is associated with reduced bilateral sensorimotor coordination and changed social interaction. Neuro ASN 1, e00013. 10.1042/an20090032 is the doi
Kim, C. H., Kim, G.-Y., Yoo, Y. H., Jeong, J. Y., Cha, H.-J., Choi, E. O., et al. (2019).
Baicalein protects HEI193 schwann cells against oxidative stress-induced DNA damage and death in part via activating the Nrf2/HO-1 signaling pathway. International. J. Med. Science. 16, 145–155. 10.7150/ijms.27005 is the doi.
Calabresi, P., Radue Ew Fau, Kappos, L., O'Connor, P., O'Connor P. Fau, Polman, C., Polman C. Fau, Hohlfeld, R., Hohlfeld R. Fau, et al. (2010). Oral fingolimod in relapsing MS patients: a placebo-controlled study. N. English. 362 (5), 387–401; J. Med. 1056/NEJMoa0909494 is the doi.
Rhie, S. J., Yoon, S., Kim, G. H., and Kim, J. E. (2015). Oxidative stress's part in neurodegenerative illnesses. Ex. neurobiology. 24, 325–340. 10.5607/en.2015.24.4.325 is the doi.
Lee, J. H., Han, D. W., and Kim, G. (2023). By preserving mitochondrial homeostasis and cellular tight connection in HaCaT keratinocytes, baicalein has cytoprotective effects on H2O2-Induced ROS. 12, 902 Antioxidants. Antiox12040902 doi:10.3390
Kipp, M., Dang, J., Copray, S., Beyer, C., and Clarner, T. (2009). The cuprizone animal model: fresh perspectives on a long-standing tale. Neuropathol Acta. 118, 723–736. 10.1007/s00401-009-0591-3 is the doi.
Bakheit, H. F., AlAli, F., Fattah, M., Alhajeri, S., Komiyama, T., Al-Kafaji, G., et al. (2022). In multiple sclerosis patients, functionally harmful mutations are found using next-generation sequencing of the whole mitochondrial genome. One 17, e0263606, PLoS. 10.1371/journal.pone.0263606 is the doi.
Kutzelnigg, A., Rauschka, H., Bergmann, M., Brück, W., Stadelmann, C., Lucchinetti, C. F., et al. (2005). Multiple sclerosis is characterized by widespread white matter damage and cortical demyelination. 128, 2705–2712; Brain. 10.1093/brain/awh641 is the doi
Bollen, A. W., Bollen Aw Fau, Atlas Sw Fau, Green, A. J., Green Aj Fau, Pelletier, D., and Langer-Gould, A. (2005). Multiple leukoencephalopathy that progresses in a patient receiving natalizumab treatment. N. English. 375–381 in J. Med. 353 (4). Reference: 10.1056/NEJMoa051847
Li, M., Cao, G. Y., Xue, W., Li, Y., Shi, A. X., Pang, H. X., et al. (2014). Pharmacokinetics, safety, and tolerability of chewable baicalein tablets given in a single ascending dosage to healthy individuals. J. ethnopharmacology. 156, 210–215. 10.1016/j.jep.2014 is the doi. 08.031
Shi, Y., Hu, R., Song, X., Xu, J., Ren, Z., Li, F., et al. (2021a). Morroniside's antioxidative stress and antiapoptotic properties, which are mediated by the PI3K/Akt pathway, shield OLN-93 cells from H2O2-induced damage. 1-675 in Cell Cycle 20. 1080/15384101.2021.1889186 is the doi.
In 2021b, Li, Y.-Y., Huang, S.-W., Pan, Z.-F., Su, Y.-L., Wang, Q., and Wang, X.-J.
By strengthening the intestinal epithelial barrier via the AhR/IL-22 pathway in ILC3s, baicalein reduces ulcerative colitis. Acta Pharmacol. Sin. 43, 1495–1507. 10.1038/s41401- 021-00781-7 is the doi
Wimmer, I., Traffehn, S., Licht-Mayer, S., Brück, W., Metz, I., Bauer, J., et al. (2015). Nrf2 expression in multiple sclerosis lesions varies by cell type. Neuropathol Acta. 130, 263–277. 10.1007/s00401-015-1452-

x is the doi.

Matute, C., and López-Muguruza, E. (2023). changes in the energy metabolism of myelin and oligodendrocytes in multiple sclerosis. International. Mol, J. Science. 24, 12912. 10.3390/ijms241612912 is the doi.

Xu, S., Hu, S., Zhang, Y., Yu, Z., Deng, M., Luo, M., et al. (2020). C57BL/6 mouse brain cells' varying susceptibilities and vulnerabilities to mitochondrial dysfunction brought on by brief exposure to cuprizone. in front. neuroanat. 14, 30. 10.3389/fnana.2020.00030 is the doi.

et al. (2018) Ma, J., Li, S., Zhu, L., Guo, S., Yi, X., Cui, T. Baicalein activates the NF-E2-related factor2 (Nrf2) signaling pathway, protecting human vitiligo melanocytes from oxidative damage. Radic Free. Biol. Med. 129, 492–503. 10.1016/j is the doi. 10.421 in freeradbiomed.2018.

Turnbull, D., Lassmann, H., and Mahad, D. (2008). Review: Multiple sclerosis's mitochondria and the course of the illness. Neuropathol. Useful. neurobiology. 34, 577–589. doi:10. 000987.x 1111/j.1365-2990.2008

Guevara, C., Orellana, J. A., Quintanilla, R. A., Ortiz, F. C., Olesen, M. A., and Maldonado, P. P. (2022). The function of Nrf2-Dependent pathways in multiple sclerosis neurodegeneration. 1146 Antioxidants. 10.3390/antiox11061146 is the doi

Biniecka, M., Veale, D. J., McGarry, T., and Fearon, U. (2018). inflammation, oxidative stress, and hypoxia. Radic Free. Biol. Med. 125, 15–24. 10.1016/j is the doi. 3.042 freeradbiomed.2018.

Šíma, M., SlanaĂ, O., and MichaliČKovÁ, D. (2020). fresh perspectives on how multiple sclerosis's compromised redox signaling interacts with inflammation and immunology. Physiology. Res. 69, 1–19. 10.33549/physiolres is the doi. 934276

Fischer, M. J. M., Olaru, O. T., Nitulescu, G. M., Ciotu, C. I., Ungurianu, A., Mihai, D. P., et al. (2021). Venlafaxine, risperidone, and febuxostat's effects on oxidative stress, behavioral abnormalities, and demyelination brought on by cuprizone. International. Mol, J. Science. 22, 7183. 10.3390/ijms22137183 is the doi

Clift, F., Lapointe, E., Schneider, R., Stefanelli, M., Devonshire, V., Morrow, S. A., et al. (2022). New information on natalizumab use in MS patients as of 2022. Mult. Scler. Relat. Strange. 65, 103995. 1016/j.msard.2022.103995 is the doi.

Kim, G.-Y., Yoo, Y. H., Park, C., Choi, E. O., Hwang, H.-J., Kim, B. W., et al. (2019). Baicalein has a protective effect on RT4-D6P2T schwann cells against oxidative stress-induced DNA damage and death. International. J. Med. Science. 16, 8–16. 10.7150/ijms is the doi. 29692

Calatayud, C. A., Bertone Uña, A. L., Millet, V., Pasquini, J. M., Soto, E. F., and Pasquini, L. A. (2006). The presence of pro-inflammatory cytokines released by microglia is necessary for cuprizone to have a neurotoxic impact on oligodendrocytes. Neurochemistry. Res. 32, 279–292. 10.1007/s11064-006-9165-0 is the doi.

Li, D. K. B., and Paty, D. W. (1993). Relapsing-remitting multiple sclerosis may be effectively treated with interferon beta-1b. Neurology 43, 662. 10.212/wnl.43.4.662 is the doi.

Hafler, D. A., and Pelletier, D. (2012). For multiple sclerosis, tingolimod. N. English.
366, 339–347; J. Med. NEJMct1101691 doi: 10.1056

Banik, N., Kurowska, E., Hogan, E., and Podbielska, M. (2013). The problem of remyelination in multiple sclerosis: myelin recovery. Brain Science. 3, 1282–1324. 10.3390/brainsci3031282 in the doi

Killestein, J., and Polman, C. H. (2006). Are anti-myelin antibodies beneficial in the treatment of multiple sclerosis? J. Neurol. neuroscience. Mental health. 77, 712. 10.1136/jnnp.2006 is the doi. 089839

Berneman, Z., Van der Linden, A., Ponsaerts, P., Praet, J., and Guglielmetti, C. (2014). The cuprizone mouse model's cellular and molecular neuropathology: clinical implications for multiple sclerosis. Neurosci. biobehaving. Rev. 47, 485–505. 10.1016/j is the doi. 2014.10.004 Neubiorev

Parisi, G., Rosito, M., Testi, C., Baiocco, P., Di Angelantonio, S., and Cortese, B. (2020). investigating the potential of dimethyl fumarate as a microglia modulator for the treatment of neurodegenerative disorders. Antioxidants 9, 700. 10.3390/antiox9080700 is the doi.

Calabresi, P. A., Calabresi Pa Fau, Stuart Wh Fau, Rudick, R. A., Galetta, S. L., Galetta Sl Fau, Radue, E.-W., Radue Ew Fau, Lublin,
F. D. and associates (2006). For relapse multiple sclerosis, natalizumab with interferon beta-1a is used.
N. English. 354, 911–923; J. Med. 1056/NEJMoa044396 is the doi.
Castelli, F., Bonina, F., Marzullo, D., Lanza, M., Scalese, M., and Saija, A. (1995). The significance of flavonoids' interaction with biomembranes as antioxidant agents. Radic Free. Biol. Med. 19, 481–486. 10.1016/0891-5849(94)00240-K is the doi
Huang, J., Xie, X., Li, Y., Ye, W., Yao, J., Shi, J., Chen, J., et al. (2023). Memory and cognitive impairments in APP/PS1 mice may be ameliorated by gut microbiota adjusted with baicalein. in front. Pharmacol. 14, 1132857. 10.3389/fphar.2023.1132857 is the doi.
Lattanzio, P., Paolicelli, D., Ruggieri, M., Signorile, A., Ferretta, A., Trojano, M., et al. (2020). The intersection of mitochondria, oxidative stress, cAMP signaling, and apoptosis in multiple sclerosis lymphocytes and the potential function of nutraceuticals. Antioxidants 10, 21. 10.3390/antiox10010021 is the doi
Sriram, S. (2011). Glial cells' function in both innate immunity and CNS demyelination. J. Neuroimmunol. 239, 13–20. 10.1016/j.jneuroim.2011.08.012 is the doi.
Tanaka, M. (2016). Varicella zoster virus infection risk in fingolimod-treated multiple sclerosis patients. Shinkeigaku Rinsho 56, 270–272. ClinicalNeurol.cn-000809 doi:10.5692

Vécsei, L., Tanaka, M., and Toldi, J. (2020). Investigating the etiological connections between bioactive kynurenines and inflammatory cytokines in neurodegenerative disorders. International.
Mol, J. Science. 21, 2431. 10.3390/ijms21072431 is the doi.
P. Theodosis-Nobelos and E. A. Rekka. (2022). Natural multi-targeting antioxidants' capacity to modulate multiple sclerosis. 27, 8402 Molecules. 10.3390/molecules27238402 is the doi.
Tobore, T. O. (2020). Moving toward a thorough pathophysiological and etiopathogenetic explanation of multiple sclerosis. International. Neurosci, J. 130, 279–300. 10.1080/00207454.2019.1677648 is the doi.
Yamamoto, M., and Uruno, A. (2023). Neurodegenerative disorders and the KEAP1-NRF2 system. antioxidant. signal of redox. 38, 974–988. 10.1089/ars.2023.0234 is the doi.
De Groot, C. J. A., and van der Valk, P. (2000). Neuropathol. Staging of Multiple Sclerosis (MS) Lesions: Pathology of the MS Time Frame. Useful. neurobiology. 26, 2–10. 10.1046/j.1365-2990.2000.00217.x is the doi.
King, R., Kaye, W., Leray, E., King, R., King, R., Rechtman, L., Marrie, R. A., et al. (2020). Globally, the prevalence of multiple sclerosis is on the rise: insights from the third edition of the Atlas of MS. Mult. Scler. 26 1816-1821. 10.1177/1352458520970841 is the doi.
Friese, M.A.-O., Woo, M.A.-O., and Engler, J.A.-O. (2024). The multiple sclerosis neuropathobiology. Nat. Neurosci, Rev. 25 (7), 493–513. 10.1038/s41583-024-00823-z is the doi.
Yang, H.-J., Li, X.-M., and Xu, H. (2013a). Antipsychotics' varying effects on the growth of cuprizone-exposed rat oligodendrocyte precursor cells. Euro. Arch. Clin. Psychiatry. Neurosci. 264, 121–129. 10.1007/s00406-013-0414-3 is the doi.
Ma, S., Liu, Q., Dang, S., Xu, J., Zhang, Y., Xiao, Y., et al. (2013b). Baicalein's inhibition of 12/15-lipoxygenase causes microglia to express PPARβ/δ, which may have therapeutic implications for CNS autoimmune diseases. Death of Cells Dis. 4, e569. 10.1038/cddis.2013.86 is the doi.
Qu, C., Zhang, J., Xu, Z., and Yan, N. (2021). Dimethyl fumarate improves cognitive deficits in chronic cerebral hypoperfusion rats by alleviating inflammation, oxidative

stress, and ferroptosis via NRF2/ARE/NF-κB signal pathway. International. immunopharmaceutical.
98, 107844. 1016/j.intimp.2021.107844 is the doi.

Yang, L., Su, Y., Guo, F., Zhang, H., Zhao, Y., Huang, Q., et al. (2020a). Deep rTMS mitigates behavioral and neuropathologic anomalies in cuprizone-exposed mice through reducing microglial proinflammatory cytokines. in front. Integrity. Neurosci. 14, 556839. 10.3389/fnint.2020.556839 is the doi.

Yang, L., Zhou, R., Tong, Y., Chen, P., Shen, Y., Miao, S., et al. (2020b). Neuroprotection by dihydrotestosterone in LPS-Induced neuroinflammation. neurobiology. Dis. 140, 104814. doi:10.1016/j.nbd.2020.104814

Zarghami, A., Li, Y., Claflin, S. B., van der Mei, I., and Taylor, B. V. (2021). Role of environmental factors in multiple sclerosis. Rev. Neurother, expert. 21, 1389–1408. doi:10.1080/14737175.2021.1978843

Zhang, L., Xu, S., Huang, Q., and Xu, H. (2017). N-acetylcysteine attenuates the cuprizone-induced behavioral changes and oligodendrocyte loss in male C57BL/ 7 mice via its anti-inflammation actions. J. Neurosci. Res. 96, 803–816. doi:10.1002/ jnr.24189

Zirngibl, M., Assinck, P., Sizov, A., Caprariello, A. V., and Plemel, J. R. (2022). Oligodendrocyte death and myelin loss in the cuprizone model: an updated overview of the intrinsic and extrinsic causes of cuprizone demyelination. Mol. Neurodegener. 17,
34. doi:10.1186/s13024-022-00538-8

Zveik, O., Fainstein, N., Rechtman, A., Haham, N., Ganz, T., Lavon, I., et al. (2022). Cerebrospinal fluid of progressive multiple sclerosis patients reduces differentiation and immune functions of oligodendrocyte progenitor cells. Glia 70, 1191–1209. doi:10.1002/ glia.24165

Zveik, O., Rechtman, A., Ganz, T., and Vaknin-Dembinsky, A. (2024). The interplay of inflammation and remyelination: rethinking MS treatment with a focus on oligodendrocyte progenitor cells. Mol. Neurodegener. 19, 53. doi:10.1186/s13024- 024-00742-8